

Towards an understanding of Type Ia supernovae from a synthesis of theory and observations

W. Hillebrandt^{1,†}, M. Kromer¹, F. K. Röpke², A. J. Ruiter¹

¹Max-Planck-Institut für Astrophysik, Karl-Schwarzschild-Str. 1, D-85741 Garching, Germany

²Institut für Theoretische Physik und Astrophysik, Universität Würzburg, Am Hubland, D-97074 Würzburg, Germany

E-mail: [†]wfh@mpa-garching.mpg.de

Received December 12, 2012; accepted January 25, 2013

Motivated by the fact that calibrated light curves of Type Ia supernovae (SNe Ia) have become a major tool to determine the expansion history of the Universe, considerable attention has been given to, both, observations and models of these events over the past 15 years. Here, we summarize new observational constraints, address recent progress in modeling Type Ia supernovae by means of three-dimensional hydrodynamic simulations, and discuss several of the still open questions. It will be shown that the new models have considerable predictive power which allows us to study observable properties such as light curves and spectra without adjustable non-physical parameters. This is a necessary requisite to improve our understanding of the explosion mechanism and to settle the question of the applicability of SNe Ia as distance indicators for cosmology. We explore the capabilities of the models by comparing them with observations and we show how such models can be applied to study the origin of the diversity of SNe Ia.

Keywords supernovae, nucleosynthesis, stellar evolution, binary and multiple stars, nuclear reactions

PACS numbers 97.60.Bw, 26.50.+x, 26.30.Ef, 26.30.-k, 97.60.-s, 97.80.-d

	Contents		4 Modeling explosion and formation of observables	124
1	Introduction	117	4.1 The MPA modeling pipeline	124
2	Observations	117	4.1.1 Hydrodynamic explosion models	124
2.1	General properties	118	4.1.2 Radiative transfer models	125
2.2	Diversity and correlations	118	4.2 Models for normal SNe Ia	126
2.3	SNe Ia and their host galaxies	119	4.2.1 Chandrasekhar-mass delayed	
2.4	Summary: Observational requirements for		detonations	126
	explosion models	120	4.2.2 Sub-Chandrasekhar-mass double	
3	Progenitors	120	detonations	128
3.1	Single-degenerate (Chandrasekhar-mass		4.2.3 Violent mergers	130
	white dwarf) scenario	121	4.2.4 Critical assessment	131
3.1.1	Hydrogen-burning donors	121	4.3 Peculiar SNe	133
3.1.2	Helium-burning donors	121	4.3.1 1991bg-like SNe	133
3.2	Double-detonation (sub-Chandrasekhar-mass		4.3.2 2002cx-like SNe	134
	white dwarf) scenario	121	4.3.3 Superluminous or “super-Chandra”	
3.3	Double degenerate mergers	122	SNe	135
3.4	Other possible scenarios	123	5 Summary and conclusions	136
3.5	Constraining progenitor models: Delay		Acknowledgements	137
	times and rates	123	References and notes	137

1 Introduction

Today, Type Ia supernovae (SNe Ia for short) play a somewhat ambiguous role in astrophysics. On the one hand, it is their relative homogeneity that caused their use as distance indicators in observational cosmology. On the other hand, this evoked an enormous interest resulting in a rather comprehensive observational survey of SNe Ia that over the last decade clearly revealed subclasses with diverging properties and variability among these objects. While the notion of homogeneity inspired the model of SNe Ia being explosions of Chandrasekhar-mass white dwarfs (WDs), the newly discovered heterogeneity of the class suggests multiple progenitors and/or explosion mechanisms.

After the pioneering work by Arnett [1] numerical simulations have been instrumental in modeling supernovae. Until the 1990s this approach was restricted to one spatial dimension which prevented a realistic treatment of the multi-dimensional burning mechanism in these objects. However, parametrized models of that time, notably the W7 model of Nomoto *et al.* [2], still set a standard in the field and are widely used in the interpretation of observational data. In the 1990s the first multi-dimensional SN Ia simulations emerged. Together with earlier work on one-dimensional models, they are reviewed by Hillebrandt and Niemeyer [3]. Here, we report on developments in the last decade, focusing on work associated with the supernova group at the Max-Planck-Institute for Astrophysics, Garching, but putting it into context with other work.

While the modeling of the explosion physics has made substantial progress (in particular with the introduction of multi-dimensional simulations), the question of the progenitor system of SNe Ia remains a fundamental problem. There is wide consensus that these events are due to thermonuclear explosions of WDs [4], most likely composed of carbon and oxygen. This was recently confirmed by Nugent *et al.* [5] and Bloom *et al.* [6] who on the basis of early time observations concluded that the exploding object in SN Ia 2011fe was a compact star. The question of how it reaches an explosive state, however, is more complicated. As single WDs are unconditionally stable, some kind of interaction with another star is necessary to explain the supernova. Unfortunately, attempts to identify this star beyond doubt have failed so far. Collisions with compact objects in globular clusters [7–9] lead to atypical events or fall short of explaining the SN Ia rate. Thus, although such events may occur in Nature, the bulk of SNe Ia is more likely to be associated with stellar binaries. The nature of the binary companion, however, is still unclear. Traditionally, two classes of potential bi-

nary progenitor systems have been distinguished – the single-degenerate progenitor channel, in which the companion is a normal star, and the double-degenerate channel with two WDs interacting and merging. At present it is unclear whether one of these possibilities is exclusively realized in Nature or whether both contribute to the class of SNe Ia.

This problem has been approached from different perspectives. Observational data becomes increasingly constraining for the physical mechanism of SNe Ia and a brief overview of the current status is given in Section 2. In addition, the rate at which SNe Ia occur and the distribution of delay times between formation of the progenitor systems and supernova explosions can help to identify the dominant progenitor channel(s). These data can be compared with predictions from binary population synthesis calculations. We discuss this approach and recent results in detail in Section 3. Another possibility is to follow different explosion scenarios in hydrodynamic simulations. Combined with radiative transfer calculations these predict observables that can be directly compared to SN Ia observations. Over the last decade substantial progress in this approach was possible due to fully multi-dimensional treatment that allows to reduce the free parameters involved in describing the physics and thus improve the predictivity of the models. We discuss recent results in Section 4, where the modeling approaches and the implementation in numerical simulations are briefly outlined followed by the presentation of models that potentially can account for normal SNe Ia (Section 4.2), while other models seem to reproduce peculiar subclasses (Section 4.3). We emphasize that this is a way of presenting our models and discussing the results. However, the assignment of models to different subclasses is not necessarily unique, but it is chosen here to point out the possibility to model a wide variety of SNe Ia when considering different progenitor scenarios and explosion mechanisms.

2 Observations

The efforts to systematically obtain observational data of SNe Ia have gained tremendous momentum during the past 15 years. This is primarily a result of their unequaled potential to act as “standardizable” candles for the measurement of the cosmological expansion rate and its variation with look-back time [10–21] (see also Goobar and Leibundgut [22] for a recent review). The discovery that the Universe entered into a phase of accelerated expansion at a redshift of around 0.5, due to the action of some unknown form of “dark energy”, was awarded with the Nobel Prize in Physics in 2011 to Saul Perlmutter,

Adam Riess, and Brian Schmidt.

For theorists, this development presents both a challenge, to help to understand the correlations among the observables, and an opportunity, to use the wealth of new data to constrain the zoo of existing explosion models. There exist a number of excellent reviews about SNe Ia observations in general [23–25], their spectral properties [26, 27], and photometry in the IR and optical bands [28–30]. Here, we highlight those aspects of SN Ia observations that most directly influence theoretical model building at the current time.

2.1 General properties

The classification of SNe Ia is based on spectroscopic features: the absence of hydrogen absorption lines, distinguishing them from Type II supernovae, and the presence of strong silicon lines in their early and maximum-light spectra, classifying them as Type Ia's [30].

The spectral properties, absolute magnitudes, and light-curve shapes of the majority of SNe Ia are remarkably similar, exhibiting only small spectroscopic and photometric differences [12]. It was believed until recently that approximately 85% of all observed events belong to this class of “normal” [32] SNe Ia, represented for example by SN 1972E, SN 1994D, or SN 2005cf. However, recent studies show that the peculiarity rate can be as high as 30% as suggested for instance by Li *et al.* [33].

The optical spectra of normal SNe Ia contain neutral and singly-ionized lines of Si, Ca, Mg, S, and O at maximum light, indicating that the outer layers of the ejecta are mainly composed of intermediate mass elements [26]. Permitted Fe II lines dominate the spectra roughly two weeks after maximum when the photosphere begins to penetrate Fe-rich ejecta [27, 34]. In the nebular phase, beginning approximately one month after peak brightness, forbidden Fe II, Fe III, and Co III emission lines become the dominant spectral features. Some Ca II remains observable in absorption even at late times [26]. The decrease of Co lines and the relative intensity of Co III and Fe III give evidence that the light curve tail is powered by radioactive decay of ^{56}Co [35] (see also Truran *et al.* [36], Colgate and McKee [37]).

The early spectra can be explained by resonant scattering of a thermal continuum with P Cygni-profiles whose absorption component is blue-shifted according to ejecta velocities of up to about $25\,000\text{ km}\cdot\text{s}^{-1}$, rapidly decreasing with time. Different lines have different expansion velocities [38–40], suggesting a layered structure of the explosion products.

Photometrically, SNe Ia rise to maximum light in a period of approximately 18 to 20 days [41–44] reaching

$$M_B \approx M_V \approx -19.30 \pm 0.03 + 5 \log(H_0/60) \quad (1)$$

with a dispersion of $\sigma_M \leq 0.3$ [45]. It is followed by a first rapid decline of about three magnitudes in a matter of one month. Later, the light curve tail falls off in an exponential manner at a rate of approximately one magnitude per month. In the *I*- and near-infrared bands, normal SNe Ia rise to a second maximum approximately 20 days after the first one [29]. Typical ^{56}Ni masses inferred from their bolometric light curves are in the range from 0.3 to $0.9 M_\odot$ for normal SNe Ia (e.g., Stritzinger *et al.* [46]).

It is especially interesting that the two most abundant elements in the universe, hydrogen and helium, so far have not been unambiguously detected in the spectra of normal SNe Ia [26, 47] (but see Meikle *et al.* [28] and Mazzali and Lucy [48] for a possible identification of He, and Hamuy *et al.* [49] and Dilday *et al.* [50] for an identification of H in individual interacting peculiar objects). Also, there are no indications yet for radio emission [51], including the rather nearby supernova SN 2011fe [52, 53].

2.2 Diversity and correlations

Early suggestions [54, 55] that the existing inhomogeneities among SN Ia observables are strongly inter-correlated are now established beyond doubt [26, 45]. Branch [12] summarizes the correlations between spectroscopic line strengths, ejecta velocities, colors, peak absolute magnitudes, and light curve shapes that were known at that time. Roughly speaking, SNe Ia appear to be arrangeable in a one-parameter sequence according to explosion strength, wherein the weaker explosions are less luminous, redder, and have a faster declining light curve and slower ejecta velocities than the more energetic events. Based on these findings Mazzali *et al.* [56] argue that a single explosion scenario, possibly a delayed detonation (see Section 4.2.1), may explain most SNe Ia. However, more recent (and better) data challenge this conclusion, as will be discussed below.

The relation between the width of the light curve around maximum and the peak brightness (brighter supernovae decline more slowly) is the most prominent of all correlations (Fig. 1; Phillips [10], Pskovskii [54]). Parameterized either by the decline rate Δm_{15} [10, 45], a “stretch parameter” [62], or a multi-parameter nonlinear fit in multiple colors [11], it was used to renormalize the peak magnitudes of a variety of observed events, substantially reducing the dispersion of absolute brightnesses (see, e.g., Leibundgut [25] and Goobar and Leibundgut [22] for recent reviews). This correction procedure is a central ingredient of all current cosmological surveys that use SNe Ia as distance indicators [63–68].

However, there are supernovae, classified as Type Ia, which violate this correlation. SN 1991bg, SN 1992K, SN

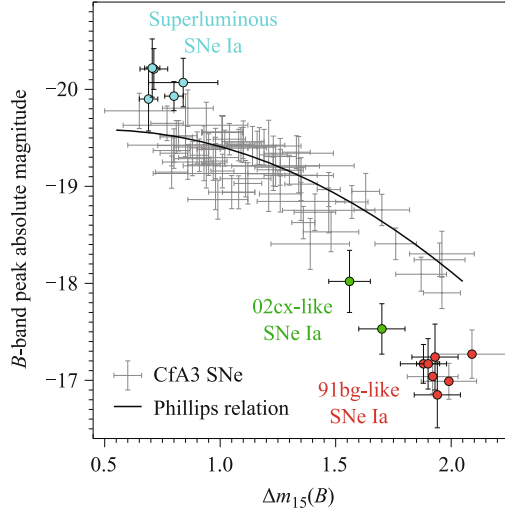


Fig. 1 Observational diversity of SNe Ia in B -band decline rate $\Delta m_{15}(B)$ and B -band peak absolute magnitude. Normal SNe Ia (shown in grey, data taken from Hicken *et al.* [57]) follow the Phillips relation [58]. 1991bg-like SNe (shown in red, data taken from Taubenberger *et al.* [59]), and 2002cx-like SNe (shown in green, data taken from Phillips *et al.* [60]) are subluminous with respect to the Phillips relation. Superluminous SNe Ia (shown in cyan, data from Taubenberger *et al.* [61]) are almost one magnitude brighter in B -band than normal SNe Ia with a comparable B -band decline rate.

1999by and SN 2005bl are well-studied examples for red, fast, and subluminous supernovae with a typical Δm_{15} value of about 1.8 and B -band peak absolute magnitudes around -17 , roughly one magnitude fainter than their “normal” counterparts [59, 69–73]. Their V , I , and R -band light curves decline unusually quickly, skipping the second maximum in I , and their spectra show a high abundance of intermediate mass elements (including Ti II) with low expansion velocities but only little iron. Models for the nebular spectra and light curve of SN 1991bg consistently imply that the total mass of ^{56}Ni in the ejecta was very low ($\sim 0.07 M_{\odot}$ [74]), a typical value for this class being $\sim 0.1 M_{\odot}$. In addition, there is also evidence for unburnt C and O in their early spectra, in contrast to normal SNe Ia. These “subluminous” explosions make up for about 15% (or more) of all SNe Ia [33].

The prototype of a second group of subluminous SNe Ia is SN 2002cx [75, 76]. Here, again, the mass of ^{56}Ni , as estimated from “Arnett’s rule” [77], is low, around $0.2 M_{\odot}$ only. The spectra show narrow lines, indicating low ejecta velocity and low kinetic energy. Other supernovae belonging to this class include SN 2005hk [60, 78], SN 2008ge [79], and SN 2009ku [80]. According to Li *et al.* [33] they contribute about 5% of all SNe Ia. Even 300 days after the explosion, the ejecta of members of this group are not transparent, but show emission from a narrow region in velocity space (less than $1000 \text{ km} \cdot \text{s}^{-1}$ [76]).

Finally, transients even fainter than 1991bg-like SNe have been observed, SN 2005E [81] or SN 2005cz [82] being examples. They are Ca-rich fast decliners, their spectra resemble more SNe Ib than SNe Ia, i.e., they show He but little O and Si in their early-time spectra, and their decline rates are similar to those of SNe Ic. They are found in old stellar populations, however, and the discussion is open whether they are thermonuclear explosions or core-collapse supernovae [83–85].

At the other end of the luminosity function, SN 1991T is often mentioned as a striking representative of bright, energetic events with broad light curves [69, 86–89]. Rather than the expected Si II and Ca II, its early spectrum displayed high-excitation lines of Fe III but returned to normal a few months after maximum light. But recently other SNe Ia were found which are even more luminous than SN 1991T, with decline rates that put them well above the Phillips relation by almost one magnitude in the B -band, prototypical examples being SN 2006gz and SN 2009dc [61, 90–94]. By now, seven objects that may belong to this subclass have been discovered and they may contribute up to about 9% of all SNe Ia [33]. In addition to their high luminosity, 2 to 3 times higher than normal SNe Ia, they are characterized by a slow decline [$\Delta m_{15}(B) \sim 0.8$], a long rise time (≥ 23 days), low ejecta velocities, and prominent C II absorption features, while other properties of their early-time spectra are similar to those of normal SNe Ia. If the luminosity at peak would come exclusively from the decay of ^{56}Ni the Ni-mass of SN 2009dc would be around 1.5 to $1.8 M_{\odot}$ [61, 95], exceeding the Chandrasekhar mass (see, however, Hachinger *et al.* [96] for an alternative scenario). The various sub-classes are illustrated in Fig. 1.

From early on, peculiar events like SN 1991T and SN 1991bg were suggested to belong to different subgroups of SNe Ia than the normal majority, created by different explosion mechanisms [69, 74, 97] although the overall SN Ia luminosity function seems to be rather smooth, with a shallow increase from an absolute R -band magnitude of -17 to -19 , followed by a steep decline to -19.5 [33] (thus leaving out 09dc-like events), indicating that “normal” SNe Ia are essentially the brightest, with Ni masses around $0.6 M_{\odot}$ while the full class may contain a large number of undetected subluminous SNe Ia.

2.3 SNe Ia and their host galaxies

There is mounting evidence that SN Ia observables are correlated with their host stellar population [12] and there are recent investigations demonstrating the dependence of supernova properties on global characteristics of their hosts [98–102]. For instance, SNe Ia in red or early-type galaxies show, on average, slower ejecta velocities,

faster light curves, and are dimmer by ≈ 0.2 to 0.3 mag than those in blue or late-type star-forming galaxies [45, 65, 98, 103, 104]. Moreover, SNe Ia seem to have lower ejecta velocity in high-mass host galaxies [105]. On the other hand side, SNe Ia at low and high redshift seem to have similar spectral evolution [106, 107].

The SN Ia rate per unit stellar mass is nearly a factor of 20 higher in late-type galaxies than in early-type ones and depends inversely on the host galaxy's mass [108–110]. The rate seems to be lower in galaxy bulges than in spiral arms. These findings indicate that there might be a population of progenitors with large delay time [111, 112]. Also, the outer regions of spirals appear to give rise to similarly dim SNe Ia as ellipticals whereas the inner regions harbor a wider variety of explosion strengths [113].

2.4 Summary: Observational requirements for explosion models

To summarize the main observational constraints, any viable scenario for the SN Ia explosion mechanism has to satisfy the following (necessary but probably not sufficient) requirements:

- Agreement of the ejecta composition and velocity with observed spectra and light curves. In general, the explosion must be sufficiently powerful (i.e., produce enough ^{56}Ni) and produce a substantial amount of high-velocity intermediate mass elements in the outer layers. Furthermore, the isotopic abundances of “normal” SNe Ia must not deviate significantly from those found in the solar system.
- Robustness of the explosion mechanism. In order to account for the homogeneity of normal SNe Ia, the standard model should not give rise to widely different outcomes depending on the fine-tuning of model parameters or initial conditions.
- Intrinsic variability. While the basic model should be robust with respect to small fluctuations, it must contain at least one parameter that can plausibly account for the observed sequence of explosion strengths. However, this could in principle also be achieved by allowing for different progenitor channels.
- Correlation with progenitor system. The explosion strength parameter must be causally connected with the state of the progenitor WD in order to explain the observed variations as a function of the host stellar population. Moreover, there must be a sufficient number of progenitor systems such that the rate and delay-time constraints are matched.

3 Progenitors

While it is widely accepted that SNe Ia originate from explosions of WDs that approach critical conditions such that burning can proceed explosively (cf. Section 1), the manner in which these conditions are achieved remains uncertain. Almost certainly the WD gains matter from a nearby stellar companion. Until very recently, the standard paradigm was the following: SNe Ia originate from probably one, possibly two different formation channels which enable the WD to reach critical conditions necessary for a thermonuclear explosion to occur (see following subsections).

However, recent observations of SNe Ia have brought to light the (previously shrouded) highly diverse nature of these objects (see Section 2). When one considers all of the necessary criteria that a progenitor model must satisfy in order to be seen as a viable progenitor candidate (robust explosion mechanism, ejecta stratification, velocities and nucleosynthesis, characteristic peak luminosity and light-curve shape, absolute birth rates and delay times), it is evident that reconciliation of the entire range of observed characteristics of SNe Ia with a single progenitor scenario is improbable. If more than one progenitor scenarios are contributing to the observed population of SNe Ia – which is currently the favoured view [114] – it is still unclear as to which progenitor scenario(s) dominate(s).

Binary population synthesis models have been used for a few decades now to estimate relative (and absolute) birthrates of various binary formation channels that can lead to SNe Ia (see Ref. [115] for one of the most well-known early studies). A powerful feature of population synthesis models is that one is able to easily compute the delay times of SNe Ia, which puts strict limits on the system age, thus ruling out certain theoretical progenitor scenarios. In addition, the models enable one to reconstruct the entire evolutionary history for all binaries of interest, which is critical for uncovering evolutionary phases (e.g. mass transfer episodes) that might give rise to observational features which could kill or confirm a given model (see e.g. Ruiter *et al.* [116] in which the STARTRACK [117] binary evolution synthesis code is used).

In terms of SN Ia rates and delay times, the results from different population synthesis codes are found to vary quite a lot in some cases and agree fairly well in others (Nelemans *et al.* [118] and references therein). This is primarily due to the rather uncertain nature of mass transfer and accretion in close binary stars which leads to differing assumptions for the input physics in the various codes. In particular, for progenitors which undergo

(quasi)stable mass exchange, one must decide how the (donor) mass transfer rate is approximated in the given binary and correspondingly, how the (accretor) retention efficiencies are computed (see, e.g., Refs. [119, 120]). Further still, the manner in which matter is lost from the binary (carrying away with it angular momentum) will also have an effect on the orbital behaviour and subsequent binary evolution [121].

The progenitor problem is still unsolved, though as previously mentioned, it seems likely that at least two progenitor scenarios (and possibly more explosion mechanisms) are required in order to explain the observed SN Ia rate and delay time distribution [122]. In the following sub-sections we review the most promising progenitor scenarios (e.g. formation channels) which are thought to lead to SNe Ia.

3.1 Single-degenerate (Chandrasekhar-mass white dwarf) scenario

3.1.1 Hydrogen-burning donors

Often called the single degenerate (SD) scenario [123], SD systems are detected in Nature (e.g. RS Oph, [124]) and were, in the past, widely thought to be the most promising SN Ia progenitors. In this scenario, the companion star is a main sequence or giant-like star (possibly a helium-burning star; see Section 3.1.2) that is overfilling its Roche-lobe, transferring matter through the inner Lagrange point in a stable manner to the companion carbon–oxygen (CO) WD. If the mass transfer proceeds within a certain range of rates (for example [125]), the donor material is accreted in a stable fashion leading to efficient hydrogen-burning (mass accumulation) on the WD, thereby increasing its (central) density. When the density in the center of a CO WD becomes high enough the carbon in the WD starts to burn (see Section 4) which eventually leads to a thermonuclear explosion, obliterating the WD and possibly imparting a significant kick on the companion star (Section 1). This critical density when carbon-burning can start is usually attained when the WD approaches a critical mass – the Chandrasekhar limit.

A typical formation pathway leading to the SD scenario involves an episode of unstable mass transfer followed by an episode of stable mass transfer at a later stage. A more specific example (e.g. Ref. [126]) is as follows: the initially more massive star (the primary) first loses its hydrogen-rich envelope on the asymptotic giant branch (AGB) when it fills its Roche-lobe and mass transfer is dynamically unstable. This results in a common envelope, which serves to bring the two stars to a smaller orbital separation [127]. The post-common enve-

lope binary comprises a (newly formed) CO WD and a (likely still on the main sequence) companion. At some later stage, the companion then fills its Roche-lobe (either while on the main sequence or as an evolved star), only this time mass transfer is stable, and the CO WD grows in mass until it approaches the Chandrasekhar limit.

3.1.2 Helium-burning donors

It is also possible that the WD may reach the Chandrasekhar mass, by accreting from a helium-burning star donor rather than a hydrogen-rich donor (e.g. Ref. [128]). Such formation channels are expected to be rare, and these progenitors have shorter evolutionary timescales than the “canonical” SD scenario due to the larger zero-age main sequence (ZAMS) mass of the secondary [126, 129, 130]. Since they might also harbour distinctly different physical (observable) properties, they have been considered their own class by some authors (e.g., helium-rich (HeR) scenario, [131]).

3.2 Double-detonation (sub-Chandrasekhar-mass white dwarf) scenario

Another progenitor channel which has recently regained popularity among the community is the sub-Chandrasekhar-mass scenario in which a sub-Chandrasekhar-mass CO WD accretes stably from a companion and never reaches the Chandrasekhar limit before exploding [129]. Depending on the assumed mass transfer/accretion rates and the mass of the CO WD, the WD is thought to be able to accumulate (rather than burn) a layer of helium which may detonate under the right physical conditions [132, 133]. This shell-detonation – if realized – likely triggers a second detonation in the sub-Chandrasekhar-mass WD, leading to a SN Ia (“double-detonation” scenario, see Section 4.2.2).

Such a scenario was investigated from a population synthesis standpoint by Tutukov and Yungelson [134] in context of helium-rich donors, and by Yungelson *et al.* [135] in context of symbiotic systems. However, formation channels leading to the double-detonation scenario via accretion from a hydrogen-rich companion are challenged by the ability of the WD to efficiently accrete (and stably burn) hydrogen and helium [136, 137]. Nonetheless, a double-detonation progenitor scenario might be readily realized in Nature from sub-Chandrasekhar-mass WDs accreting from helium-burning stars or helium-rich degenerate (or semi-degenerate) stars [134, 138].

In considering all potential helium-rich donors transferring mass to sub-Chandrasekhar-mass CO WDs, Ruiter *et al.* [131] investigated the double-detonation sce-

nario. In that work, two characteristic evolutionary channels were found (note that the authors only considered SNe Ia to arise from systems where the total WD mass was $\gtrsim 0.9 M_{\odot}$). The typical formation channels were as follows:

Helium-burning star donors. This formation channel involves two cases of unstable mass transfer (common envelopes) followed by a later stage of stable mass transfer from the secondary to the CO WD. The initial primary star fills its Roche-lobe (unstably) while on the AGB when the companion is still on the main sequence, resulting in a CO WD–main sequence binary. A second common envelope ensues when the secondary star – now evolved – fills its Roche-lobe. The post-common envelope binary consists of a CO WD (left over from the first common envelope) and a stripped core of a giant; a compact naked helium-burning star. Since the stars are already on a fairly close orbit (due to two common envelopes), it does not take long for the stars to be brought into contact. The naked helium-burning star then fills its Roche-lobe and transfers matter stably to the primary WD, until the onset of the double-detonation.

(Semi-)degenerate star donors. A number of evolutionary pathways can lead to the formation of such a progenitor, but the most common path also involves two common envelopes (primary on the AGB, then secondary on the giant branch), followed by a phase of stable mass transfer. However, in this case, the secondary’s ZAMS mass is smaller than that of helium-burning star donor case. Thus, when the secondary loses its H-rich envelope in the second common envelope, a degenerate (non-burning) naked helium core of a giant is left behind. Once contact is achieved, the “helium-rich WD” transfers matter stably to the CO WD until the onset of the double-detonation.

3.3 Double degenerate mergers

Another scenario which might readily lead to SNe Ia is the merger of two CO WDs where the total mass exceeds the Chandrasekhar limit (“double degenerate” (DD) scenario, [139]). Along with the SD scenario, the DD scenario has been a leading progenitor candidate model. The reason is owed partially (but not only) to the theoretical birth rate calculations – for which it historically does the best of any progenitor scenario. A number of population synthesis studies over the last few decades (e.g. Ref. [115]) have demonstrated that mergers of CO WDs with a total mass exceeding the Chandrasekhar limit might be frequent enough to account for Galactic SN Ia rates, depending on e.g. the adopted prescriptions for common envelope evolution [126, 140]. Still, when considering *cosmological* SN Ia rates as a function of delay time, the

DD model scenario, like other scenarios, often falls short of the observationally-recovered rates by at least a factor of a few [131, 141, 142]. However, some of the most recently-measured delay time distributions indicate that DD merger rates might indeed be frequent enough to account for the bulk of SNe Ia at least in some stellar populations ([110, 116], see Section 3.5).

There are a number of progenitor pathways that can lead to a CO-CO WD binary. A typical one would be the following [126]: The primary star fills its Roche-lobe when it is slightly evolved, and mass transfer is stable to the companion (a second stable phase of Roche-lobe overflow may follow a bit later, when the primary is an evolved helium star). The primary star then evolves into a CO WD. The secondary star fills its Roche-lobe when it is an evolved star but mass transfer is unstable to the WD, and a common envelope ensues. The post-common envelope binary consists of a CO WD and a naked helium-burning star. Following this, a final phase of stable mass transfer may occur whereby the slightly evolved helium star (secondary) transfers matter to the primary WD. Such a final phase of mass transfer was found to be important in explaining the peak-brightness distribution of SNe Ia (see Section 4.2.4). Once the WDs reach contact and the larger (less massive) one fills its Roche-lobe, mass transfer must be unstable for a merger to occur. This is the likely outcome for double CO WDs given their typical mass ratios (see Ref. [143]; see also Toonen *et al.* [141] for specific examples of DD formation channels).

Despite favourable theoretical rate predictions, the DD scenario has received a lot of criticism over the years. Earlier calculations predicted that the likelihood of thermonuclear explosion in a double CO WD merger is rather unlikely. Such a merger ($M_{\text{tot}} \gtrsim M_{\text{Ch}}$) was thought to lead to disruption of the secondary WD which is then accreted onto the primary. The accretion would not lead to central burning but rather burning in the outer layers of the WD, where densities are lower, and the accreting CO WD would transform into an oxygen-neon-magnesium WD [144]. For WDs of such composition, electron captures become important at high central densities, and as the WD approaches the Chandrasekhar mass it collapses to form a neutron star in an accretion-induced collapse (AIC, [145]). Even if DD mergers do lead to SNe Ia, it has been reiterated by some groups that, assuming the estimated birthrates from population synthesis calculations are correct within a factor of a few, all CO WD mergers (even those with $M_{\text{tot}} < 1.4 M_{\odot}$) must lead to SNe Ia in order to match the observed rates [146, 147]. It is unclear whether lower-mass mergers lead to thermonuclear explosions, let alone if such explosions would produce enough ^{56}Ni .

Depending on the configuration of the binary system – in particular the mass ratio – the merger may be somewhat quiescent as described above, or it may be violent enough such that a prompt detonation in the primary WD will occur. These “violent mergers” are robustly found to lead to a thermonuclear explosion, and they are described in Section 4.2.3.

3.4 Other possible scenarios

Other possible formation channels leading to SNe Ia have been postulated in the literature. For example: a potential scenario involves the merger of a CO WD and the core of an AGB star during a common envelope event [148, 149]. Such events are expected to readily occur, however it is unclear whether such “core-degenerate” mergers would lead to an immediate (or delayed, [150]) explosion that exhibits observational signatures which match those of SNe Ia.

3.5 Constraining progenitor models: Delay times and rates

The delay time distribution (DTD) is the distribution of times in which SNe Ia explode following a (hypothetical) burst of star formation. Knowing the DTD gives the age of the progenitor, which places strong constraints on the different proposed progenitor scenarios. If the SN Ia rate is known in addition, then it becomes possible to rule out theoretical formation channels.

Calculation of observationally-recovered DTDs involves many assumptions, the most important being the assumed star formation history of the supernova’s host galaxy or local stellar population, for which several techniques have been employed [110, 151]. There are two emerging facts in the literature: i) there is a population of “prompt” SNe Ia which have delay times $\lesssim 500$ Myr and seem to comprise a significant fraction of all SNe Ia, and ii) there are SNe Ia which are “delayed”, the seemingly-continuous DTD spanning up to a Hubble time, with a characteristic (cosmic) DTD beyond > 400 Myr that follows a power-law shape $t^{-1.2}$ [142]. Such a power-law ($\sim t^{-1}$) is expected if the dominating timescale leading to SNe Ia is set by gravitational radiation, as is the case for DD mergers [152].

With binary population synthesis models, the entire evolutionary history of each binary is followed, so the DTD is easily determined for all potential SN Ia progenitors. In Fig. 2 we show mass-normalized theoretical DTDs for the following progenitor scenarios: SD (hydrogen-burning and helium-burning donors); a subclass of the DD, whereby the mass of the primary WD must be $\geq 0.8 M_{\odot}$ and there are additional restric-

tions on the mass ratio, (cf. Section 4.2.3); and double-detonation progenitors involving both helium-burning star and helium-rich WD donors [116, 126, 131]. Alongside our theoretical DTDs we show the most recent DTDs from (red squares, Maoz *et al.* [153]) and the best-fit DTD from observations as described in Graur and Maoz [110] (t^{-1} power-law best-fit). All of the DTDs are normalized per mass formed in stars, and can be thought of as an absolute SN Ia rate as a function of Hubble time. We note that the observational DTDs, while currently the most recently-derived, have amplitudes that are at least a factor of a few lower than cosmic DTDs derived from previous studies (see Maoz *et al.* [153] for discussion).

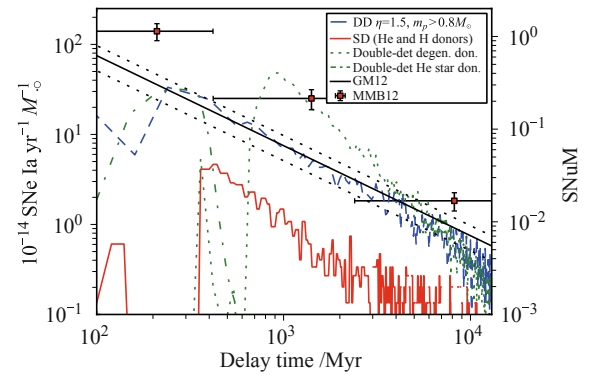


Fig. 2 Coloured lines show STARTRACK theoretical delay time distributions from 100–13000 Myr after star formation assuming a 70 % binary fraction. The DTDs have been mass-normalized into units of $\text{SNe Ia } (10^{10} M_{\odot})^{-1} (100 \text{ yr})^{-1}$. The lines have been smoothed, and small fluctuations are due to Monte Carlo noise. *Dashed blue*: DD violent WD mergers, which are a DD scenario sub-class (cf. Section 4.2.4); *solid red*: SD Chandrasekhar-mass scenario including main sequence, giant-like and helium-burning donors; *green dotted*: double-detonation scenario (see also Ref. [131]) with helium-rich WD donors; *green dash-dotted*: double-detonation scenario with helium-burning star donors. Alongside the model DTDs, we show the recent observationally-recovered DTD from Maoz *et al.* [153] (red squares) and the DTD from observations as described in Graur and Maoz [110] (straight black lines; t^{-1} best-fit).

It is immediately obvious that no single progenitor channel can reproduce the observed rates for delay times < 300 Myr. The SD (red, solid line) “spike” at delay times < 200 Myr is solely due to helium-rich donors; these donors have relatively faster evolutionary timescales than their hydrogen-donor SD counterparts (hence the gap $\sim 200 - 300$ Myr). The SD DTD drops off too quickly to follow a t^{-1} power-law, but shows the expected trend at delay times > 400 Myr (decreasing events with increasing delay time). Overall, the SD rates are too low by about an order of magnitude to match the observed SN Ia rate.

The double-detonation progenitors display a clear bimodal behaviour: prompt events originate from systems

with helium-burning star donors (green dash-dotted line; short evolutionary timescales) while delayed events originate from systems where the donor is a degenerate dwarf (green dotted line; longer evolutionary timescales). Beyond ~ 300 Myr, the rates match the observations fairly well, and beyond 1 Gyr the DTD follows a (steeper) power law $\sim t^{-2}$ (see also Ref. [131]). However, there is still a lot of uncertainty with respect to the explosion mechanism of this channel regarding the detonation of the helium shell (Section 4.2.2).

The sub-set of DD mergers shown in Fig. 2 – a population of violent mergers (blue dashed line) – are discussed in detail in Ruiter *et al.* [116] (see also Section 4.2.3). Once a double WD is born, it may take several Gyr before the stars are brought into contact. The dominant mechanism leading to a decrease in orbital angular momentum (and hence smaller orbit) is the emission of gravitational waves [154]. As is expected, the DD mergers shown here follow the t^{-1} power-law shape fairly well, and are within the observational uncertainties for delay times > 300 Myr (below 300 Myr there is a dip in the distribution, see Section 4.2.4 for explanation). It may also be possible to increase the overall rates of DD mergers if three-body interactions are taken into account [155].

4 Modeling explosion and formation of observables

4.1 The MPA modeling pipeline

A thorough testing of different SN Ia scenarios requires to combine several model aspects from progenitor evolution over the explosion to the formation of the observables. A way of addressing the progenitor problem was discussed in Section 3. Here we present our approaches to modeling hydrodynamics and nucleosynthesis in the thermonuclear explosion and radiative transfer in the ejecta cloud giving rise to the observables. In the subsections which follow we first describe our combustion-hydrodynamic code LEAFS and then the Monte-Carlo radiative-transfer code ARTIS.

4.1.1 Hydrodynamic explosion models

Type Ia supernova explosion models aim at following the hydrodynamical evolution from the ignition of thermonuclear burning in a WD to homologous expansion of the ejecta. These models rely on the equations of hydrodynamics (either the Euler equations or specific approximations suitable for low-Mach number flows) coupled to nuclear reactions. After ignition, a combustion wave forms. Because of the high temperature sensitivity of car-

bon fusion, it is confined to a narrow region in space. Seen from the scales of the WD, it can be approximated as a sharp discontinuity separating the fuel (CO material) from the ashes of the nuclear burning. The reactive Euler equations allow (in their integral form) for two distinct classes of discontinuous (weak) solutions that model the propagation of such thin combustion waves: subsonic *deflagrations* and supersonic *detonations*. Microscopically, the deflagration propagation mode corresponds to a flame mediated by heat conduction, while a detonation is driven by a shock wave.

The most critical aspect in modeling thermonuclear explosions of WDs are the inherent scale problems – both in time and space. Although in large-scale simulations of supernova explosions that capture the entire WD star it is well justified to treat the combustion fronts as discontinuities (at least for most of the burning taking place at high fuel densities), this implies that the internal structure of the flame cannot be resolved. Thus, details of their mechanism and in particular the nuclear reactions are not represented. A time scale problem is the discrepancy between the scales of hydrodynamic flows and that of the nuclear reactions. In Chandrasekhar-mass models, the ignition of the combustion wave is preceded by a period of convective carbon burning (the so-called “simmering phase”) that lasts for a century and is characterized by highly turbulent flows. A correct modeling of turbulence is also essential for deflagration phases in Chandrasekhar-mass explosion models. Here, Reynolds numbers of the order of 10^{14} are typically encountered posing another severe spatial scale problem.

While a detailed modeling of the ignition process and the simmering phase in Chandrasekhar-mass explosion models remains challenging (but see Refs. [156, 157] for recent efforts), there have been several attempts to overcome the spatial scale problem associated with combustion fronts. In large-scale supernova simulations, an option is to artificially broaden the combustion waves so that they can be represented on the computational grid. This flame-capturing approach was explored by Khokhlov [158, 159]. The main drawback is that an artificially-broadened flame smears out small-scale dynamics. Level-set based techniques for combustion wave tracking are an alternative which has been introduced to SN Ia simulations by Reinecke *et al.* [160, 161]. The underlying idea is to represent a contour (in 2D simulations) or a surface (in 3D simulations) by the zero-level set of a scalar field that is set up as a signed distance function to the combustion wave. This scalar field is then evolved in an appropriate way to model the propagation of the burning front [160]. In this approach, the combustion wave is considered as a sharp discontinuity and no attempt is made to resolve its inner structure. It there-

fore has to be augmented by a model for the propagation speed of the combustion wave and the energy release in it. For deflagrations, the laminar flame speed has been determined in small-scale simulations [162]. This sets the lower limit of the propagation speed of the effective flame front in large-scale supernova simulations. For most of the time, turbulence determines the flame speed and this is accounted for by a specific modeling approach (see below). For detonations, the propagation speed in the most simple case is the Chapman–Jouget speed, i.e., the sound speed in the ashes. This, however, does not take into account the dependence on shock strength and possible multi-dimensional effects. In addition, at high densities burning to nuclear statistical equilibrium makes part of the process endothermic and pathological detonations are encountered here. For these, the microscopic mechanism has been studied by Sharpe [163] and the results can be used to model the propagation of detonations in large-scale supernova simulations.

The available computational resources limit the reaction networks employed in the hydrodynamic explosion simulations to only a few species. This allows to represent the energy release to a sufficient precision to account for its impact on the dynamics of the explosion. The detailed nucleosynthetic yields, however, cannot be determined directly. These are required to compare the models with the constraints from galactic chemical evolution and for setting the input models for radiative transfer simulations that rely on a spatially resolved multi-dimensional chemical structure of the ejecta. This problem is usually accounted for by a nucleosynthetic postprocessing step [164, 165]. In the hydrodynamic explosion model, a large number (up to several million) of Lagrangian tracer particles are advected with the flow. They represent fluid packages and for these the thermodynamic trajectories are recorded. These data are then used as input for a large reaction network that allows to reconstruct the details of the nuclear reactions.

Finally, the expansion of the WD and the ejecta in the course of the explosion pose another scale problem. With ejecta velocities well above $20\,000\text{ km}\cdot\text{s}^{-1}$ the material would quickly leave a static computational grid. Two approaches to overcome this problem are followed. Adaptive mesh refinement allows to use large computational domains with finer resolution at places where physical processes are to be resolved. An alternative, which is implemented in our models, is to use moving computational meshes [166–168]. As the overall expansion of the ejecta is spherical to first order, a simple radial expansion of the computational grid provides an optimal resolution of the explosion physics with given computational resources and allows for following the hydrodynamic evolution of the ejecta to a relaxed state (homologous expansion) –

a prerequisite for predicting observables with radiative transfer simulations.

4.1.2 Radiative transfer models

From the hydrodynamic explosion simulations we obtain the velocities, densities and composition of the explosion ejecta. These, however, are not directly comparable to the observational signatures of SNe Ia like broad-band photometry, spectral time series and spectropolarimetry over a wide range of the electro-magnetic spectrum. For that purpose synthetic spectra and light curves must be obtained from radiative transfer calculations. Since the explosion ejecta are free streaming at about 100s after the explosion (e.g. Ref. [166]), the radiative transfer calculations can be decoupled from the hydrodynamic simulation assuming homologous expansion of the ejecta.

The observational display of SNe Ia is not powered by the heat produced during the explosion itself. Already at the first observational epochs, typically a few hours to days after the explosion, this heat has long gone due to the expansion of the ejecta. Instead, the decays of radioactive isotopes like ^{56}Ni and ^{56}Co , freshly synthesized during the thermonuclear burning, give rise to the emission of a spectrum of γ -photons. These interact with the ejecta by Compton scattering, pair production and photoelectric absorption, thereby depositing their energy and reheating the ejecta [36, 37]. Thus, radiative transfer simulations that aim at a direct connection between explosion models and observations have to take into account this energy injection and the transport of γ -photons explicitly. A simple photospheric assumption (e.g. Ref. [169]) is not enough.

Another complication poses the peculiar chemical composition of SNe Ia. Since their ejecta do not contain any hydrogen but significant amounts of iron-group elements, the opacity in SN Ia is dominated by the wealth of lines associated with the iron-group elements (e.g. Ref. [170], Fig. 1), thus requiring a solution of the complicated multi-line transfer problem in expanding media. Assuming emission from a photosphere and spherical symmetry, many studies have addressed this problem in the past either assuming pure resonance scattering (e.g. Ref. [169, 171, 172]) or pure absorption (e.g. Ref. [87]) in the lines. However, such an approach is too simple, since it cannot account for line fluorescence effects which are crucial in shaping the spectral energy distribution of SNe Ia [170, 173].

Finally, given the complex ejecta structure of state-of-the-art hydrodynamic explosion models a time-dependent 3D “full-star” treatment of radiative transfer which simulates the γ -deposition and spectrum formation in detail is needed. Such an approach is e.g. taken

in the Monte Carlo radiative transfer code SEDONA of Kasen *et al.* [174] which treats line fluorescence in an approximate way similar to [170, 173].

Following the methods outlined by Lucy [175–177], at MPA we have developed another time-dependent 3D Monte Carlo radiative transfer code ARTIS [178, 179]. ARTIS divides the total energy available in the radioactive isotopes of a given supernova model into discrete energy packets. These are initially placed on a computational grid according to the distribution of the radioactive isotopes and then follow the homologous expansion until they decay. Upon decay they convert to bundles of monochromatic γ -ray photons which propagate through the ejecta. ARTIS contains a detailed treatment of γ -ray radiative transfer [180] and accounts for interactions of γ -ray photons with matter by Compton scattering, photo-electric absorption and pair production. Assuming instantaneous thermalization of absorbed γ -ray photons, the energy is transformed into ultraviolet-optical-infrared photons enforcing statistical and thermal equilibrium. Using a detailed wavelength-dependent opacity treatment, ARTIS solves the radiative transfer problem self-consistently with the ionization and thermal balance equations. Excitation is treated approximately by assuming local thermodynamic equilibrium, which is expected to be a good approximation at least around maximum light. A generalized treatment of line formation [175, 176], including typically about 500 000 individual atomic line transitions [181] in the Sobolev approximation [182], allows for a detailed treatment of radiation-matter interactions including a parameter-free treatment of line fluorescence. Thus, depending only on the input model and atomic data, our radiative transfer calculations give a maximum of predictive power for a given explosion model.

4.2 Models for normal SNe Ia

As discussed in Section 2, normal SNe Ia can be explained by the decay of typically $0.3 M_{\odot}$ to $0.9 M_{\odot}$ of ^{56}Ni in the center of the ejecta which is surrounded by layers of intermediate mass elements, oxygen and unburnt material. There are several ways of constructing explosion models that give rise to such an ejecta structure.

4.2.1 Chandrasekhar-mass delayed detonations

The model of a WD exploding when approaching the Chandrasekhar mass is certainly the most thoroughly explored option. Traditionally, it is associated with the single-degenerate progenitor model (see Section 3), but the formation of a Chandrasekhar-mass WD due to a merger is not excluded. A strong argument in favor of the

Chandrasekhar-mass model was the notion of homogeneity among SNe Ia. This picture, however, eroded with the detailed observational campaigns of the past decade (see Section 2) that clearly showed a pronounced diversity among these objects. By now, several sub-classes have been established. Therefore, it seems unlikely that all SNe Ia can be explained within a single progenitor/explosion model. Nonetheless, from the explosion modeling point of view, the Chandrasekhar-mass scenario holds promise to explain the bulk of normal SNe Ia. There may, however, be difficulties with explaining the rate of observed events, when this scenario arises exclusively in the single-degenerate channel (see Section 3).

One-dimensional parametrized models of explosions in Chandrasekhar-mass WDs have been very successful in reproducing normal SNe Ia, most notably the W7 model of Nomoto *et al.* [2]. Here, we will focus on recent developments in simulating the nuclear burning in two or three spatial dimensions. There is a qualitative difference between such models and earlier one-dimensional parameterizations. On the one hand, multidimensional approaches allow for a more realistic treatment of inherently multidimensional effects such as turbulent burning and asymmetries in the ignition and flame propagation. On the other hand, by fixing free parameters, such models cannot easily be used to fit observations and thus the level of agreement with observations is usually lower. Thus, the assessment on the validity of the underlying models is more involved and interpretation is required.

The first numerically studied explosion model, a *prompt detonation of a Chandrasekhar-mass WD* [1] can be ruled out as an explanation for SNe Ia. Since detonations propagate at supersonic velocities with respect to the fuel, there is no causal contact between the energy release and the material ahead of the combustion wave. Thus, the entire star burns at the high initial densities (a few times 10^9 g/cm^3) of a Chandrasekhar-mass WD in hydrostatic equilibrium. Consequently, burning proceeds to nuclear statistical equilibrium (complete burning) throughout most parts of the star and the ejecta consist almost exclusively of iron group elements (predominantly ^{56}Ni). This is in conflict with the observational requirements for normal SNe Ia, see Section 2. In order to produce less ^{56}Ni and a substantial amount of intermediate mass elements, at least parts of the burning must proceed at lower densities than those encountered in Chandrasekhar-mass WDs in hydrostatic equilibrium.

A combustion starting out in the deflagration mode brings the WD out of equilibrium and pre-expands the fuel material. Consequently, burning partially takes place at lower densities than in an equilibrium Chandrasekhar-mass WD. This allows for the synthesis of intermediate-

mass elements and reduces the ^{56}Ni yield accordingly. However, ultimately laminar deflagration flames are too slow to catch up with the expansion of the star. This limits the amount of material burnt and thus the nuclear energy release is too low for a successful SN Ia. It has been noted early on [2] that deflagrations will not propagate at their laminar speeds. Burning from the WD's center outward, they produce an inverse density stratification in the gravitational field of the star and it is thus subject to buoyancy instabilities. The Rayleigh–Taylor instability and secondary shear instabilities generate strong turbulence. Driven from large scales, the turbulent energy cascades down to the microscopic Kolmogorov scale. Consequently, the flame interacts with turbulent eddies of various sizes. The flame is torn and wrinkled by these turbulent motions and this enlargement of the flame surface area accelerates its mean propagation significantly.

Several numerical studies indicate that although turbulence is driven on large scales by buoyancy, it quickly becomes isotropic and follows Kolmogorov-scaling at smaller scales [183, 184]. The correct representation of flame-turbulence interaction is one of the key challenges in modeling deflagrations in WDs and thus a critical ingredient in Chandrasekhar-mass models for SNe Ia. Several possibilities have been suggested to accomplish this. In the work discussed here, a subgrid-scale model is employed. It is based on a balance equation for the unresolved turbulent kinetic energy. For two-dimensional simulations, the approach of Niemeyer and Hillebrandt [185] is used while three-dimensional simulations use the method of Schmidt *et al.* [186] that does not make any assumptions on the scaling of turbulence. For strong turbulence, as expected for most phases of the supernova explosion, flame-turbulence interaction implies that on some sufficiently large scale (such as resolved in multi-dimensional simulations) the propagation speed of the effective flame (averaged over unresolved small-scale structure) decouples from the laminar burning speed and is set by the turbulent velocity fluctuations on that scale [187]. This is the basis for the flame model in our simulations that employ the level-set technique to represent the effective deflagration front and use a subgrid-scale turbulence model for determining its effective propagation velocity (for details see also Ref. [188]).

The amount of burning and the energy release depend strongly on the way the flame is ignited. In Chandrasekhar-mass explosions a century of convective carbon burning precedes the actual flame ignition (cf. Section 4.1.1). Numerical simulations of this phase are extremely challenging due to its long duration and the high turbulence intensities involved (but see [156, 189, 190] for recent attempts). At the moment, the geometry of flame ignition is unclear and therefore different possi-

bilities are considered. If ignited in many sparks around the center, the WD can be unbound [168, 191]. But even with a strong ignition, the asymptotic kinetic energy of the ejecta does not exceed $\sim 0.6 \times 10^{51}$ erg and the ^{56}Ni production reaches at best about a third of a solar mass [191]. The most optimistic values for pure deflagrations in Chandrasekhar-mass WDs reach the fainter end of *normal* SNe Ia, but they cannot account for all of them. Moreover, the predicted spectra show peculiarities that can be attributed to a chemically mixed ejecta composition which is a natural consequence of the large-scale buoyancy instabilities in these models. Thus we conclude that deflagrations in Chandrasekhar-mass WDs cannot explain *normal* SNe Ia. They could, however, account for a peculiar subclass (see Section 4.3.2).

The only chance for Chandrasekhar-mass explosion models to reach the ballpark of *normal* SNe Ia is a detonation following the initial burning in the deflagration mode. In contrast to a prompt detonation of a Chandrasekhar-mass WD in hydrostatic equilibrium, the pre-expansion in the deflagration phase now allows the detonation to burn at lower fuel densities. Although it still can contribute to the overall ^{56}Ni production, it produces a substantial layer of intermediate mass elements in the outer layers of the exploding WD. One way to realize this is the *delayed-detonation scenario* [194], in which a spontaneous transition of the burning front from deflagration to detonation occurs in a late stage of the explosion. This leads to a clear chemical stratification with iron group elements dominating the inner part of the ejecta while the products of a detonation in material of subsequently lower density lead to a stratified composition in the outer layers. Here, intermediate-mass elements follow the iron group elements and at higher velocities oxygen and carbon dominate. Downdrafts of unburned material left behind in the turbulent and unstable deflagration are now incinerated. A qualitative difference to earlier one-dimensional delayed-detonation models, however, is that stable iron group elements produced in the high-density deflagration at the center of the WD do not stay there but float to larger radii due to buoyancy instabilities. The degree of the pre-expansion and thus the total ^{56}Ni production is determined by the energy release in the deflagration [56, 195] and by the delay between deflagration ignition and detonation triggering. One way to vary the strength of the deflagration is by choosing different ignition configurations (although other parameters may also affect the strength of the deflagration phase, see e.g. Refs. [196–199]). Igniting vigorously in many ignition sparks around the WD center (e.g., Refs. [168, 200]) releases more energy in the deflagration burning, hence achieving more pre-expansion [56, 195], while a sparse and perhaps asymmetric ignition leads

to a weak deflagration phase (e.g., Refs. [201, 202]). In the context of the delayed-detonation explosion scenario this gives rise to a variability of ^{56}Ni production which, in turn, leads to a range in brightnesses of the simulated events covering that of *normal* SNe Ia. The brightness of the faintest model is set by the strongest pre-expansion and thus by the most vigorous deflagration that is achievable. For nearly isotropic ignitions with standard WD setups this corresponds to a ^{56}Ni production in the range of $[0.3 \cdots 0.4] M_{\odot}$ – clearly too much for subluminal SNe Ia. On the other end, weak deflagrations arising from asymmetric ignitions easily lead to the production of up to a solar mass of ^{56}Ni in the delayed-detonation scenario. Thus, in principle, this model should be able to reproduce the range of observed brightnesses of normal SNe Ia.

As an example, Fig. 3 shows model N100 [192, 193] which is ignited in 100 ignition sparks around the center. The ensuing deflagration (left panel) is of intermediate strength. The middle panel shows the deflagration front directly prior to the first deflagration-to-detonation transition. The large-scale buoyancy-induced plumes of burnt material are clearly visible. This – together with shear-induced turbulence on smaller scales leads to the increase in flame surface area characteristic for the turbulent deflagration. The panel on the right hand side shows a snapshot shortly after the first deflagration-to-detonation transition has triggered. Obviously, it is immediately followed by other transitions at different locations. The newly formed detonation waves quickly spread over the remaining fuel and burn out the down-drafts of fuel material left behind from the deflagration. Since the detonation propagates from high to low density the ash composition changes from iron-group to intermediate-mass nuclei and, because of the supersonic propagation, there is no mixing, in contrast to the deflagration phase. The outcome is an ejecta cloud with a stratified chemical composition in the outer layers and

close to $0.6 M_{\odot}$ of ^{56}Ni at the center. The hydrodynamic evolution is followed with a moving-grid technique to 100 s after ignition. After nucleosynthetic postprocessing, the ejecta structure is mapped into the radiative transfer code ARTIS [178, 179] to calculate synthetic observables. A sequence of spectra for this model is shown in the left panel of Fig. 4. Overall, the agreement between the model spectra and the observational reference spectra of a normal SN Ia (SN 2005cf) is reasonable. Again, we emphasize that no perfect match is expected in this comparison of a generic three-dimensional supernova model and an observation without any attempts of fitting. However, a more fundamental shortcoming of the model is that it appears to be too red. This can be attributed to a flux redistribution due to stable iron group elements at rather high velocities – a feature that at least to a certain degree is characteristic for delayed-detonation models.

A more systematic test has been presented by Kasen *et al.* [203] on the basis of a suite of two-dimensional models. Again, although no perfect agreement with observational data is reached, many of the models would be classified as SNe Ia employing a tool for analyzing observations and treating the models as actual astronomical data [204]. However, the brightest and most asymmetric explosions in the Kasen *et al.* [203] sample would not be classified as SNe Ia. Interestingly, in this set of models, the correlation between peak luminosity in the *B*-band and the decline rate of the light curve (used to calibrate SNe Ia as distance indicators in observational cosmology, [10, 58]) was found to resemble that of the observations [203]. Whether or not this is the case also in sets of three-dimensional models remains to be seen and is subject to forthcoming publications (Sim *et al.*, in preparation).

4.2.2 Sub-Chandrasekhar-mass double detonations

The observational finding of chemically stratified ejecta

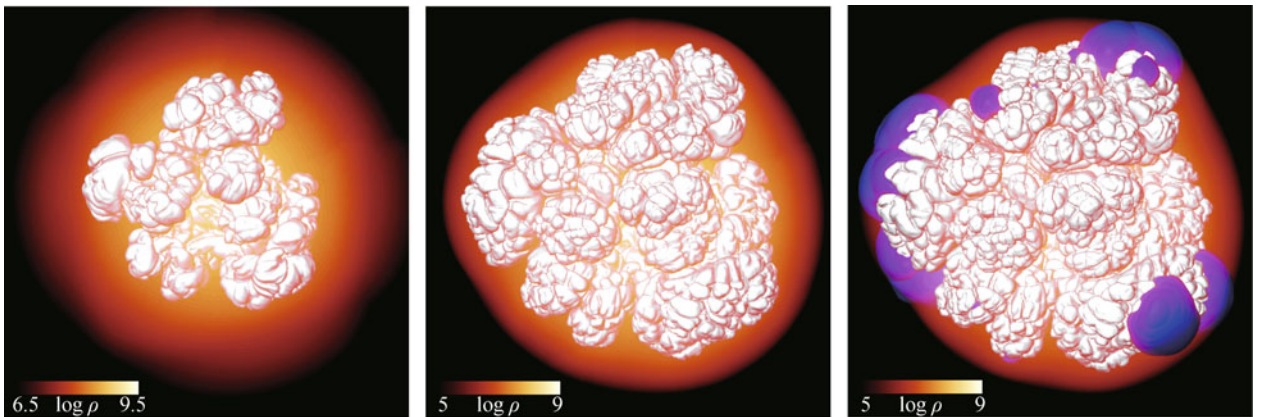


Fig. 3 Hydrodynamic evolution of a Chandrasekhar-mass delayed detonation. Shown are a volume rendering of the density (orange colours) and the zero level-set of the deflagration (whitish surface) and detonation flames (blueish colours) of model N100 [192, 193]. From left to right the snapshots are taken at 0.70, 0.93 and 1.00 s.

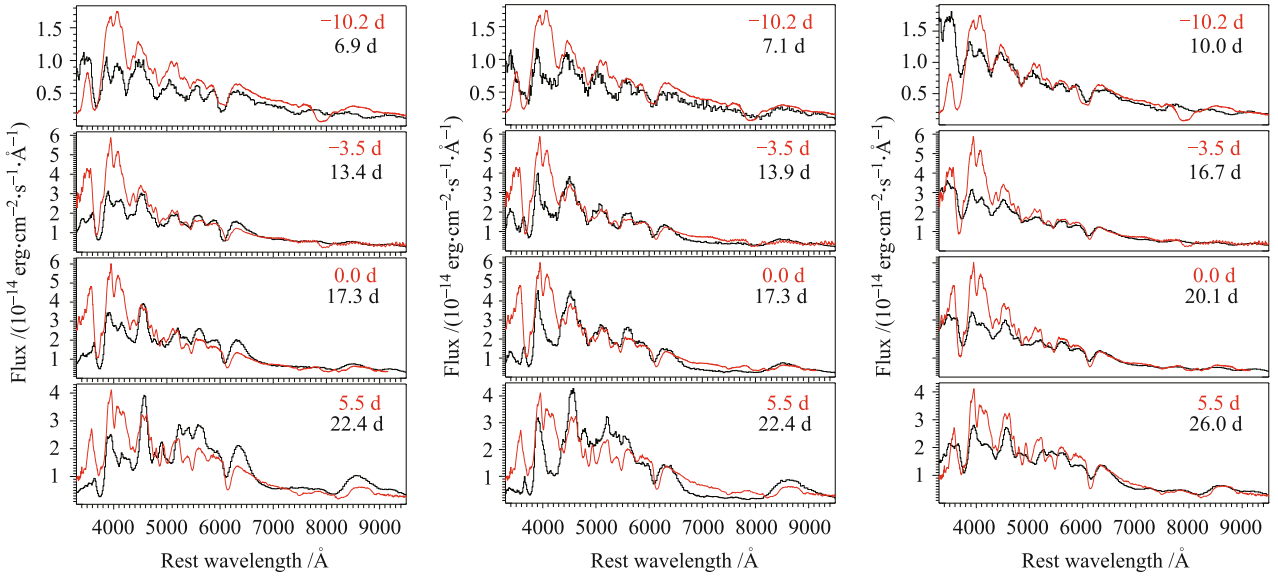


Fig. 4 Synthetic spectra of different kinds of explosion models for normal SNe Ia. From left to right the panels show (i) the delayed-detonation model N100 [192], (ii) model 3m of the sub-Chandrasekhar-mass double detonations presented by Kromer *et al.* [205], and (iii) a double-degenerate merger of two WDs with 1.1 and $0.9 M_{\odot}$ [206]. For comparison, we show observed spectra of the “golden-standard” normal SN Ia 2005cf for corresponding epochs [40] (data in red).

points to a detonation propagating down the gradient towards low densities in the outer layers of the exploding WD. As discussed above, for Chandrasekhar-mass WDs this is only compatible with a configuration that is out of hydrostatic equilibrium. An alternative to this mechanism is a detonation in a sub-Chandrasekhar mass WD. Pure detonations in CO WDs with masses between $0.81 M_{\odot}$ and $1.15 M_{\odot}$ have been tested by Sim *et al.* [207] (see also Shigeyama *et al.* [208]) and yield ^{56}Ni masses in the range of $[0.01 \dots 0.81] M_{\odot}$. According to the model sequence of Sim *et al.* [207], a standard normal SN Ia with $\sim 0.6 M_{\odot}$ of ^{56}Ni is expected to result from a detonation in a WD of about $1.1 M_{\odot}$. The observables predicted from these models roughly match the data from normal SNe Ia and their *B*-band light curves seem to follow the width-luminosity relation [207]. Thus, detonations in WDs with masses well below the Chandrasekhar-limit hold promise for explaining normal SNe Ia. The question is how a detonation in such an object can be triggered. Here we discuss one possibility arising from a detonation in an accreted He shell on top of the WD. Another possibility – due to the merger of two WDs – will be presented in the next section.

The idea of double detonations in sub-Chandrasekhar mass WDs has been discussed extensively in the 1990s by Woosley and Weaver [209], Livne and Arnett [210], Benz [211], Livne [212], García-Senz *et al.* [213]. A CO WD accretes helium from a companion star (either a helium star or a helium WD). When the accreted He layer becomes sufficiently massive, compressional heating is thought to lead to a detonation in the He material (see, however, [214] for an alternative mechanism based

on instabilities in the accretion process). This detonation sweeps around the CO core and burns the He to heavier elements. At the same time a shock wave propagates into the core. This shock may trigger a secondary detonation close to the interface between the CO core and the He shell (“edge-lit detonation”), or when reaching the center of the core. The secondary detonation incinerates the entire WD and leads to its successful disruption in a thermonuclear supernova. The question, however, is whether the event would really look like a SN Ia. Although for sufficiently massive CO cores enough ^{56}Ni can be produced to power a normal SN Ia, problems arise from the burning products of the He shell. In the models of the 1990s, a rather massive He shell – about $[0.1 \dots 0.2] M_{\odot}$ – was thought to be necessary to trigger a detonation and to drive a sufficiently strong shock wave for initiating a secondary detonation in the core. In such massive He shells, a detonation produces a significant fraction of iron group elements (including additional ^{56}Ni). These affect the radiative transfer and the predicted observables are at odds with the actual observations [215–218].

Recently, however, Bildsten *et al.* [220] and Shen and Bildsten [221] pointed out that in AM CVn systems rather low masses of accreted He on top of a CO WD can develop dynamical burning, possibly in the detonation mode. The work by Fink *et al.* [219, 222] demonstrated that a core ignition is very robust due to spherical shock convergence near the center of the WD which leads to a geometrical shock amplification. Neither asymmetric ignition geometries [222] nor low He shell masses prevent a secondary core detonation once the He shell successfully triggers a detonation [219]. The low He shell mass

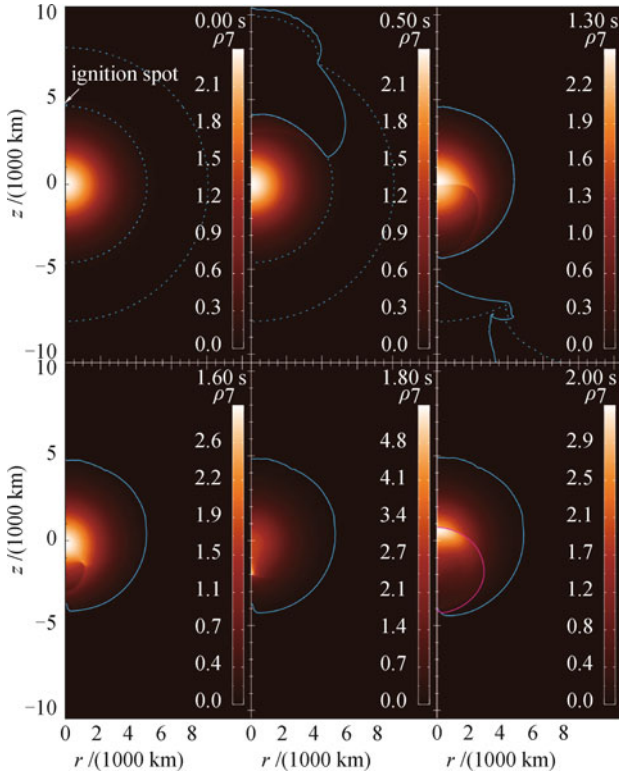


Fig. 5 Hydrodynamic evolution of a sub-Chandrasekhar-mass double detonation for a helium shell of $0.084 M_{\odot}$ on top of a $0.920 M_{\odot}$ CO WD (from top left to bottom right; model 2 of Fink *et al.* [219]). The density structure of the WD is colour coded in red (ρ_7 in units of 10^7 g cm^{-3}). The dashed blue lines indicate the border of the helium shell. The solid blue and magenta lines show the helium and CO detonation flames, respectively.

significantly reduces the observationally disfavored effects of iron group elements in the outer layers of the ejecta [205]. In addition to lowering the total mass of the He shell, it also reduces the density at which He detonates thus leading to predominantly incomplete burning. Consequently, the outer layers of the ejecta in the models of Fink *et al.* [219] contain virtually no ^{56}Ni and only low amounts of other iron group elements. Another effect that distinguishes the models of Fink *et al.* [219] from many earlier calculations and also from the recent models of Woosley and Kasen [218] is the multi-dimensional treatment of the He shell detonation. Sweeping around the CO core, it propagates laterally and allows for significant post-shock expansion – an effect that is not captured in spherically symmetric models. This adds to the less complete burning observed in the simulations of Fink *et al.* [219] (see also Ref. [223]). According to Kromer *et al.* [205] the reduced yields of heavy elements from the He detonation have significant impact on the predicted observables. Although the colors are too red to match the observations perfectly, the range of brightnesses and rise and decline rates of normal SNe Ia is covered by the models.

Kromer *et al.* [205] also point out that the details of spectra and the colors are very sensitive to the thermal and chemical conditions in the detonating He shell. In particular, they find that the degree of burning in the shell material (and thus its final composition) can be affected by the initial composition of the He shell. Since the time-scale for α -captures behind the detonation shock front is significantly shorter than that of triple- α reactions, a ^{12}C admixture in the He shell due to previous hydrostatic burning or dredge-up of core material [221] can limit the α -chain before reaching nuclear statistical equilibrium. In an exploratory model Kromer *et al.* [205] homogeneously polluted a He shell with 34% (by mass) of ^{12}C (their model 3m) and showed that such a model produces light curves and spectra that are in good agreement with those of normal SNe Ia. In particular, this model is no longer too red at maximum light. However, one caveat remains: the model still produces a non-negligible amount of Ti in the outer layers leading to the formation of a Ti II absorption trough between 4000 \AA and 4400 \AA which is not observed in normal SNe Ia (see also middle panel of Fig. 4) but in subluminous 91bg-like supernovae only (Section 2.2). Whether these differences can be resolved as well, remains to be seen in future studies that more fully explore the influence of the initial composition of the helium shell and different ignition geometries. Also the strong sensitivity of the radiative transfer to tiny amounts of particular elements requires a better description of nuclear reaction rates and continued study of the radiative transfer processes (and atomic data) in order to quantify more fully the systematic uncertainties which arise due to the complexity of spectrum formation in supernovae.

4.2.3 Violent mergers

Another external trigger to ignite a sub-Chandrasekhar-mass WD is the violent merger of two CO WDs. Although the total mass of the merging system usually exceeds the Chandrasekhar mass, both components are below this mass limit. The so-called *violent merger model* [224] starts with massive WDs ($M \gtrsim 0.9 M_{\odot}$) with a mass ratio close to unity. This scenario results from a subset of double-degenerate progenitor models. Other configurations of merging WDs may avoid thermonuclear explosions (e.g., Ref. [225]) and instead lead to the formation of a neutron star by gravitational collapse [144].

For mass ratios close to unity, however, the mergers proceed dynamically and can be followed in hydrodynamic simulations. Pakmor *et al.* [206] studied the merger of a $1.1 M_{\odot}$ “primary” WD with a $0.9 M_{\odot}$ “secondary” WD. The inspiral and merger, as followed with the SPH code GADGET [226] in its modification for stel-

lar astrophysical problems [227] is shown in Fig. 6. In the last few orbits before the actual merger, tidal interaction strongly deforms the secondary and it finally plunges into the primary WD (snapshots for $t > 600$ s in Fig. 6). This violent merger leads to the formation of a hot spot where the two masses collide (marked by a black + in the snapshot for $t = 610$ s). Here, thermodynamic conditions are suitable for triggering a detonation.

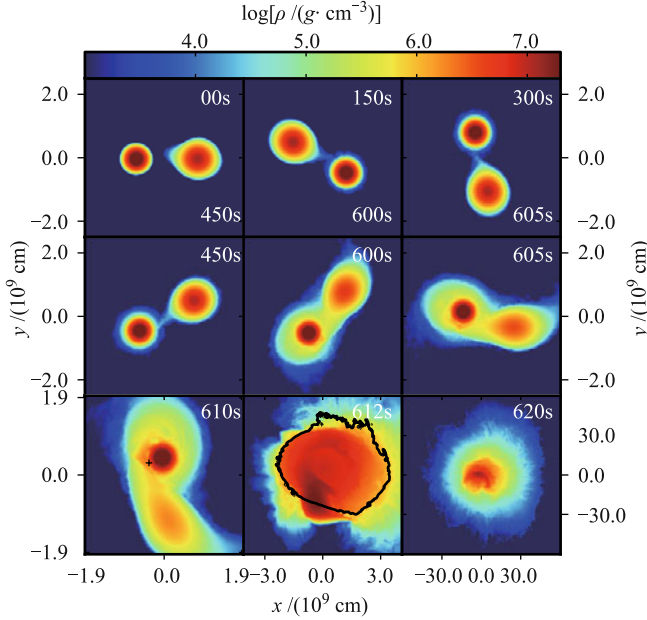


Fig. 6 Hydrodynamic evolution and subsequent thermonuclear explosion of a merger of a pair of 1.1 and $0.9 M_{\odot}$ WDs [206]. Initially the WDs orbit each other with a period of ~ 35 s. After a few orbits the secondary is tidally disrupted and collides with the more massive primary reaching densities and temperatures sufficient to ignite a detonation at 610 s (black cross). At 612 s the detonation front (black line) has burned almost the complete object. Color-coded is the logarithm of the density. Note that the last two panels have a different color scale ranging from $10^{-4} \text{ g} \cdot \text{cm}^{-3}$ to $10^6 \text{ g} \cdot \text{cm}^{-3}$ and $10^4 \text{ g} \cdot \text{cm}^{-3}$, respectively.

After mapping into our grid-based supernova explosion code, the detonation (indicated by a black contour in Fig. 6) is followed with the level-set technique (see Section 4.1.1). It incinerates the merged object almost completely. An important point to notice is that the primary WD is nearly unaffected by the merger. Therefore the burning takes place at the low densities typically found in sub-Chandrasekhar-mass WDs. Only the primary possesses material at sufficiently high densities to synthesize iron group elements while the secondary mostly burns to oxygen. With the mass of the primary chosen to $1.1 M_{\odot}$, a moderate ^{56}Ni mass production is expected according to [207] and indeed $0.64 M_{\odot}$ of ^{56}Ni are found in the presented simulation. Significant amounts of the total $2 M_{\odot}$ of material involved in this merger burn to intermediate-mass elements ($0.6 M_{\odot}$) and the ejecta contain $0.47 M_{\odot}$ of oxygen. Only $0.09 M_{\odot}$ of carbon remain in the ejecta.

Thus, despite the large total mass of the exploding object, the angle-averaged and line-of-sight dependent light curves of this merger compare very favorably to that of normal SNe Ia. With a peak brightness of -19.6 , -19.0 , and -19.2 in the U , B , and V bands, respectively, and a B -band light curve decline rate of $\Delta m_{15}(B) = 0.95$, the model predictions are well in the range of those observed for normal SNe Ia [57]. Moreover, the spectral evolution of the model (see Fig. 4) reproduces the overall spectral shape and the velocity-shifts of most of the line features remarkably well and shows most of the characteristic features of SNe Ia, particularly the defining Si II doublet at $\lambda\lambda 6347, 6371$ but also the weaker Si II features at $\lambda\lambda 5958, 5979$ and $\lambda\lambda 4128, 4131$. Other prominent features are the Ca II H and K absorptions, the Mg II triplet at $\lambda 4481$, the Si II W-feature at $\sim 5400 \text{ \AA}$ and, in the red tail of the spectrum, the O I triplet $\lambda\lambda 7772, 7774, 7775$ and the Ca II NIR triplet. However, with a B -band rise time of 20.8 d the pre-maximum light curve evolution of this merger model is relatively long compared to that of normal SNe Ia. Hayden *et al.* [44], for example, find an average B -band rise time of 17.4 d in the SDSS-II SN sample (but see also Conley *et al.* [43] who find a value of 19.58 d for a low red-shift sample from the SNLS). This could indicate that the total ejecta mass in this model is somewhat too large. Future studies exploring the parameter space of violent WD mergers in more detail will show if this explanation is right.

4.2.4 Critical assessment

Although the models presented above produce successful explosions that overall compare favorably to the observations of normal SNe Ia, there remain uncertainties in the modeling of the explosion physics. In all models this refers to the initiation of the burning and the formation of detonations. This is not too surprising as these processes work on scales that cannot be resolved in our multi-dimensional supernova simulations. Moreover, the ignition of deflagrations and detonations are complex physical phenomena and their microphysics not completely understood, even for terrestrial combustion. Despite our attempt to model the explosion physics as parameter-free as possible, we are thus left with the following critical points in the three classes of models:

- *Delayed detonations in Chandrasekhar-mass WDs* hinge on the possibility of deflagration-to-detonation transitions to occur in WD combustion. Although some recent studies (e.g., Refs. [228–231]) indicate that this may indeed be the case, it is difficult to definitely decide on its realization in SNe Ia. The other major uncertainty in this model is

the way the deflagration ignites. A strongly asymmetric ignition leads to extremely bright events in the context of delayed detonations. Reaching the low-luminosity end of the normal SNe Ia requires to limit the ^{56}Ni production to the yield of the strongest pure deflagrations. These result from quasi-isotropic or central ignitions of the WD – a scenario that is currently not favored by ignition simulations [156] but may arise due to slight rotation in the ignition phase [190].

- *Double detonations in sub-Chandrasekhar mass WDs* require the initiations of two detonations. While the secondary detonation in the CO core seems to be virtually unavoidable [219, 222], the initial detonation in the He shell is not established beyond doubt – in particular for the case of low He-shell masses.
- *Violent mergers of two WDs* rely on the triggering of a detonation at the encounter of the two stars. Although the simulations of Pakmor *et al.* [206, 224, 232] indicate that this is possible, the mechanism still awaits a firm proof.

A better understanding of the microphysics of thermonuclear combustion is thus required to overcome these uncertainties and to assess the models purely from the plausibility of their explosion mechanism. This is a challenging task and a convincing result is not expected in the short term. There are, however, alternative ways to judge the potential of different explosion scenarios to account for the majority of normal SNe Ia.

One possibility, which we followed here, is to perform supernova simulations under the assumption that the uncertain mechanisms in the modeling proceed in a favorable way and to compare the outcome with observations. Our results indicate that all of the models considered here are able to cover the range of explosion energies and brightnesses of normal SNe Ia and to first order reproduce their light curves and spectra relatively well. The comparisons of our synthetic spectral time series and SN 2005cf in Fig. 4 demonstrate this success, but also show that in detail there are shortcomings in each of the models as discussed in the previous sections. In the Chandrasekhar-mass delayed-detonation and sub-Chandrasekhar-mass double-detonation models the blue-shift of the characteristic Si II is too large compared to SN 2005cf, indicating slightly too high ejecta velocities. This potentially can be cured by more realistic progenitor models with carbon-depleted cores [192]. Moreover, the models are too red compared to the observations. This is most pronounced for the delayed-detonation Chandrasekhar-mass model but also found in the double-detonation sub-Chandrasekhar-mass and the

violent merger model to some degree.

Although the involved masses and the explosion physics of the models shown in Fig. 4 differ significantly, at the current precision of the models it is difficult to distinguish them by means of maximum-light optical spectra only. This degeneracy prevents favoring one model over others. This could imply that all channels contribute to normal SNe Ia (possibly with different realization frequencies) or other ways of discriminating them have to be found. Promising for this task seem observations in the ultraviolet (e.g., Refs. [105, 233]) and in the near-infrared bands (e.g., Ref. [234]) but also late time observations (e.g., Refs. [192, 235]), spectropolarimetry (e.g., Refs. [236, 237]) or gamma-ray observables (e.g., Refs. [180, 238, 239]). For these, either theoretical models have yet to be developed for modern multi-dimensional SN Ia simulations, or data has to be acquired.

Other possibilities to discriminate different explosion scenarios are the search for signatures of the progenitor system in nearby SNe Ia (see, e.g., Refs. [5, 6, 33, 52, 53, 240, 241] for observational constraints and, e.g., Refs. [242–245] for theoretical predictions) or in supernova remnants (e.g., Refs. [246–249]).

Finally, any model scenario that is claimed to account for a large fraction of SNe Ia must be able to explain observational trends like e.g. the observed delay-time and brightness distribution of SNe Ia. By combining the synthetic observables from our explosion models with studies of the realization frequency of the supposed progenitor systems, as discussed in Section 3, we can thus put additional constraints on the different explosion scenarios.

Recently, we have used this approach to investigate the prospect of the violent merger scenario in more detail. As was noted in Section 4.2.3, the secondary WD in a violent merger – while consumed in the explosion – does not contribute to synthesizing ^{56}Ni . Thus, it is the primary WD (more specifically its mass) that simply determines the peak luminosity of a SN Ia in the violent merger model.

For a realistic estimate of primary WD masses in would-be merging WD pairs, we took the distribution of primary WD masses of all merging CO WDs from the binary evolution population synthesis calculations of Ruiter *et al.* [131] (their standard model). Using this mass distribution, a relationship between the (primary, sub-Chandrasekhar mass) WD and its corresponding SN bolometric peak brightness ($m_{\text{WD}} - M_{\text{bol}}$) was derived using the technique as described in Sim *et al.* [207].

One critical question is the realization of a WD merger itself: e.g. what is the critical mass ratio for which mass transfer will be dynamically unstable (and lead to a merger) when the larger WD fills its Roche-lobe? The

answer to this question is not straightforward, and much uncertainty exists in the modeling of mass transfer in close binaries [250]. A trend that was found in the merger simulations of Pakmor *et al.* [206] (see also Ref. [251]) is that the critical mass ratio q_c likely decreases with larger primary masses. We constructed a relationship [[116], Eq. (1)] that follows this trend to evaluate whether a given double WD could produce a merger that is sufficiently violent. Additionally, for the violent WD mergers we limited the primary mass to be above $0.8 M_\odot$ since primaries less massive than this are expected to barely produce even $0.01 M_\odot$ of ^{56}Ni ([207], Table 1).

Figure 7 shows four model (bolometric) peak brightness distributions for a range of q_c -cuts. In grey scale we over plot the (scaled-up) observational luminosity distribution of SNe Ia from Li *et al.* [33]. Regardless of the assumed q_c -cut, our theoretical brightness distributions do a fairly good job in covering the range and matching the shape of the observed SN Ia brightness distribution. Such good agreement indicates that merging WDs which explode via the violent merger mechanism could be dominant SN Ia progenitors, driving the shape of the underlying brightness distribution.

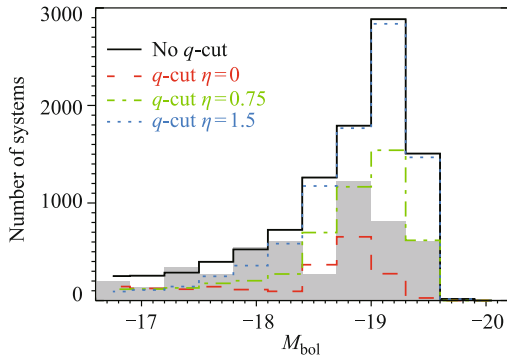


Fig. 7 Brightness distribution of violent WD mergers [see Ref. [116], for details]. Black solid histogram shows *all* CO WD mergers from population synthesis, while coloured histogram lines show the brightness distributions when more stringent mass ratio constraints are assumed. Grey scale shows the observational peak brightness distribution of 74 SNe Ia from the volume-limited sample of Li *et al.* [33]; observations are scaled up to enable comparison with the distribution shapes from our models.

In Fig. 8 we show the primary mass in the same model for violent WD mergers as a function of delay time. The darkest hexagons represent the regions of highest density for a given cell. It is clear from the plot that mergers hosting the most massive primaries ($\gtrsim 1.3 M_\odot$) tend to merge at prompt (< 500 Myr) delay times. (We note that in single star evolution, CO WDs would not achieve such high masses and a WD of mass $\sim 1.3 M_\odot$ would be composed mostly of oxygen and neon. However, in binary evolution, such masses are allowed for CO WDs, in particular if the CO WD accretes mass after it has

formed (see e.g. Ref. [116], Fig. 2)). Since in the violent merger model the SN Ia luminosity is determined by the primary WD mass, this means that we would expect the brightest SNe to be found amongst very young stellar populations; a trend which is confounded by observations [252]. One aspect of the binary evolution model which remains to be confirmed, is whether or not primary WDs are able to efficiently accrete on the order of $0.2 M_\odot$ from a slightly-evolved helium star companion. Such a mass transfer phase was found to be critical in producing a large number of primary WD masses that yield peak explosion brightnesses around -19 mag (see Ref. [116]). Additionally, we note that there exists another population of violent mergers with very short (< 100 Myr; ultra-prompt) delay times. These systems undergo two common envelope phases, whereby the secondary star loses its envelope twice.

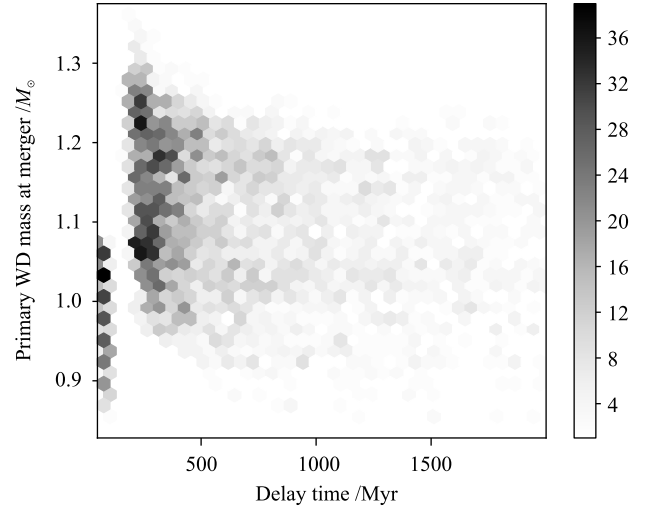


Fig. 8 Delay time distribution for primary WD masses at time of merger for one of our violent merger model populations (cf. blue histogram in Fig. 7). We show delay times only from 0–2000 Myr so that the characteristic primary masses at prompt delay times are clearly visible. The most massive primaries tend to merge at delay times < 400 Myr, however there also exists a distinct population of “ultra-prompt” mergers with less-massive primaries with delay times < 100 Myr (see text).

4.3 Peculiar SNe

As discussed in Section 2.2, as of today several peculiar sub-classes of SNe Ia have been found in addition to the bulk of spectroscopically normal SNe Ia which follow the Phillips relation. Here, we discuss possible explosion models for a few of those peculiar sub-classes.

4.3.1 1991bg-like SNe

1991bg-like SNe are subluminous with respect to the Phillips relation and peak at about -17 mag, indicating that only a rather low ^{56}Ni mass of about $0.1 M_\odot$

was synthesized during the explosion. Moreover, a spectral analysis of SN 2005bl, a well-observed proto-typical 1991bg-like SN, has shown that both iron group elements and silicon are present over a wide range of radii extending down to very low expansion velocities. This indicates the presence of incomplete Si burning over a wide velocity range in these explosions as it may occur in detonations at low densities.

In the violent merger scenario (see also Section 4.2.3 [224]) such a burning is possible for a primary WD with a sufficiently shallow density profile. Following the inspiral of a pair of $0.89 M_{\odot}$ WDs with the SPH code GADGET and using our full modeling pipeline Pakmor *et al.* [224] have shown that such a configuration produces about the right amount of ^{56}Ni although a total mass of $1.8 M_{\odot}$ is involved in the merger. Moreover, their simulation can reproduce the observed spectra and light curves of 1991bg-like SNe (see Fig. 9) and accounts for most of their peculiar features.

Pakmor *et al.* [232] find that WD binaries with a primary mass of $M_1 \sim 0.9 M_{\odot}$ and mass ratios $q = M_2/M_1 > 0.8$ evolve similarly, thus confirming a robust ignition of $\sim 0.9 M_{\odot}$ violent WD mergers which makes them promising candidates for 1991bg-like SNe given the good agreement of synthetic observables in our pilot study. Arguing that primary WDs with a lower mass will not detonate due to their lower densities and using population synthesis calculations of Ruiter *et al.* [126], Pak-

mor *et al.* [224] also estimated the rate of binary mergers that met the necessary criteria to satisfy their model. It was found that such mergers may contribute on the order of 2%–11% to the total SN Ia rate, which is not too far off from the observationally derived rate for 1991bg-likes of 15% [33]. Moreover, if the WD binaries undergo only one common envelope phase and/or begin their evolution on the ZAMS with wide orbital separations their model also prefers old (> 1 Gyr) stellar populations as indicated by observations of 1991bg-like SNe.

4.3.2 2002cx-like SNe

One of the most peculiar sub-classes of SNe Ia are explosions similar to SN 2002cx [75]. Those events are underluminous with respect to the Phillips relation and their NIR light curves do not show secondary maxima. Moreover, their spectra are characterized by very low expansion velocities compared to normal SNe Ia and show signs of strongly mixed ejecta. While explosion models involving a detonation are not able to explain such an ejecta structure (e.g., Refs. [193, 207]), turbulent deflagrations in Chandrasekhar-mass WDs naturally predict such a strong mixing and low kinetic energies [256, 257].

Given our ignorance of the exact ignition configuration of Chandrasekhar-mass WDs (see Section 4.2.1), we have recently performed a systematic study of 3D full-star explosion simulations of pure deflagrations in

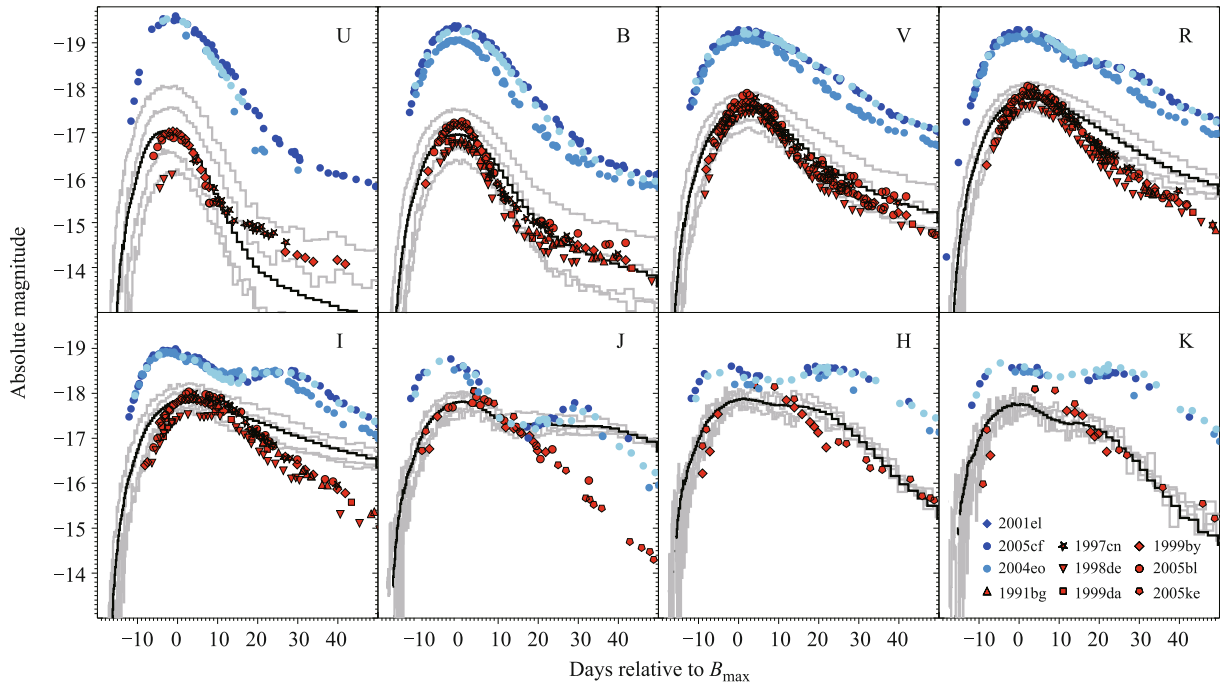


Fig. 9 Angle-averaged synthetic light curves of a merger of two $0.89 M_{\odot}$ WDs (black). To indicate the spread due to different viewing angles, the gray lines show light curves along four different lines-of-sight. These have been selected from 100 equally sized solid-angle bins such that they represent the full range of the scatter. For comparison observed photometry for normal (blueish colours, Krisciunas *et al.* [253], Pastorello *et al.* [254, 255]) and sub-luminous 1991bg-like SNe (red, Taubenberger *et al.* [59] and references therein) is shown.

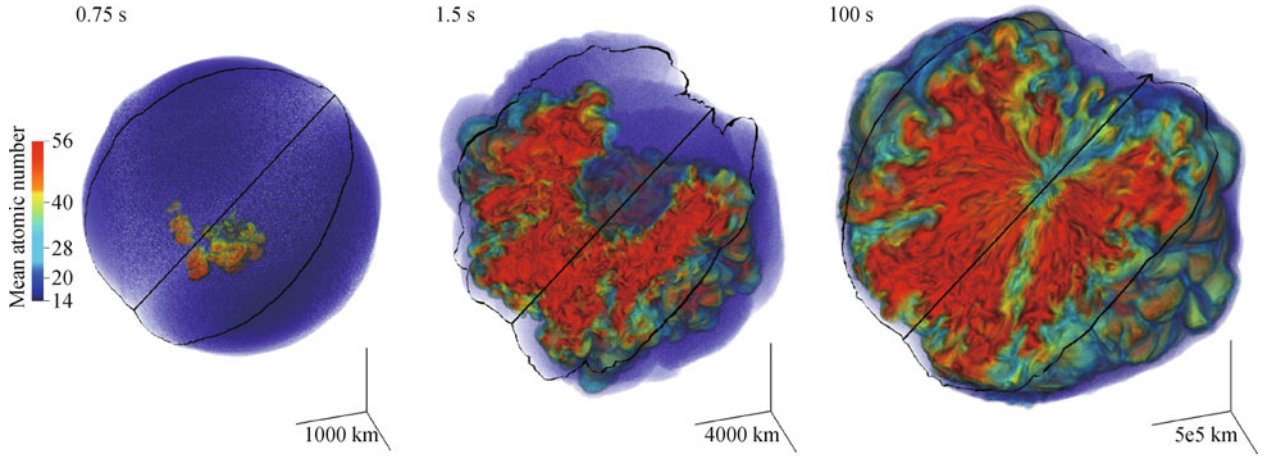


Fig. 10 Hydrodynamic evolution of an asymmetrically ignited deflagration in a Chandrasekhar-mass WD. Particularly we show model N5def of Fink *et al.* (in preparation) which ejects about $0.37 M_{\odot}$ of which $\sim 0.16 M_{\odot}$ are ^{56}Ni . Shown is a volume rendering of the mean atomic number (colour bar) from which we carved out a wedge to allow a view into the core. At 0.75 s after the explosion a one-sided deflagration plume rises towards the WD surface which fragments due to buoyancy instabilities. (ii) At 1.5 s the expansion of the WD quenches the burning and the explosion ashes wrap around the unburned core. (iii) Finally, at 100 s the unburned core is completely engulfed by the explosion ashes which are accelerated to escape velocity.

Chandrasekhar-mass WDs (Fink *et al.*, in preparation) for different ignition setups. Depending on the strength of the ignition which is parametrized by a varying number of ignition sparks to seed unstable burning modes we obtain ^{56}Ni masses between 0.035 and $0.38 M_{\odot}$. Moreover, we find that only strong ignitions release enough energy during the burning to unbind the progenitor WD completely. Asymmetric, weak ignition setups, in contrast, lead to a one sided deflagration plume which fragments due to Rayleigh–Taylor and Kelvin–Helmholtz instabilities and finally wraps around the still unburned WD core when it comes close to the surface (Fig. 10; see also Refs. [201, 258]). However, even deflagrations which fail to unbind the complete WD accelerate parts of their explosion ashes to escape velocity and eject this material into their surroundings.

Using a million Lagrangian tracer particles, we determined the detailed chemical composition of our simulations from a post-processing calculation with our 384-isotopes nuclear network [164, 165] and mapped the resulting ejecta structure into our radiative transfer code ARTIS [178, 179]. While the obtained synthetic observables for strong deflagrations, which completely unbind the progenitor WD, do not match the display of observed SNe, deflagrations which leave behind a bound remnant closely resemble the observed properties of 2002cx like SNe (Fig. 11, for details see Kromer *et al.* [259] and Jordan *et al.* [260]).

4.3.3 Superluminous or “super-Chandra” SNe

Recently observations revealed a new class of superluminous SNe Ia (e.g., Refs. [61, 90]) with total ejecta masses

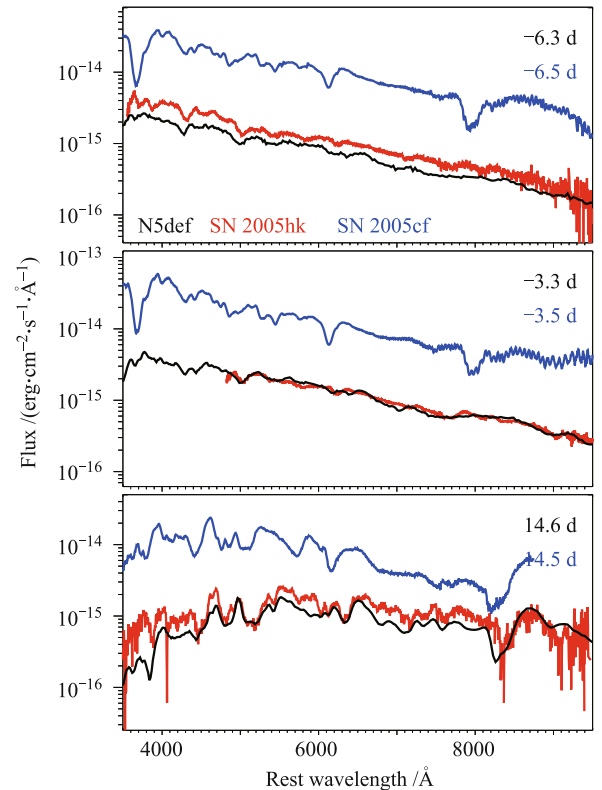


Fig. 11 Synthetic spectra of the asymmetrically ignited deflagration model N5def which leaves behind a bound remnant. The spectral evolution is remarkably similar to SN 2005hk [60], a prototypical 2002cx-like SN. For comparison we show also spectra of SN 2005cf [40] as an example for a normal SN Ia.

significantly larger than the canonical Chandrasekhar mass of $1.4 M_{\odot}$. SN 2009dc, which is one of those objects, requires even a ^{56}Ni mass larger than the Chandrasekhar mass if its peak luminosity was solely powered

by radioactive decay of ^{56}Ni and its daughter nuclei [61, 95]. One model which was proposed for these peculiar objects by Howell *et al.* [90] is that of exploding rapidly rotating WDs which stay stable well above $1.4 M_{\odot}$ due to centrifugal forces [261].

Several authors have studied prompt detonations [262, 263] and turbulent deflagrations [264] in such differentially rotating WDs. Here we report on a *delayed detonation in a differentially rotating WD* of $2 M_{\odot}$ (see Fig. 12; Fink *et al.*, in preparation). Compared to a delayed detonation in a non-rotating WD, the initial deflagration propagates preferentially along the rotation axis since angular momentum conservation and weaker gradients in the effective potential inhibit the growth of flame instabilities in lateral directions. A similar effect was already found by Pfannes *et al.* [264] for pure deflagrations in such an object. As a consequence not much energy is released during the deflagration phase. Therefore, the WD does not expand strongly before the deflagration-to-detonation transition leaving a large amount of fuel at high densities which the ensuing detonation efficiently burns to nuclear statistic equilibrium.

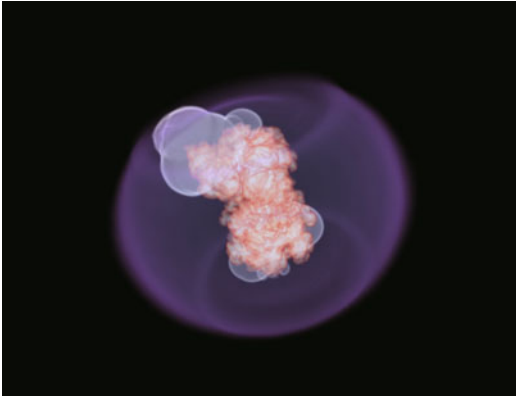


Fig. 12 Delayed detonation in a differentially rotating WD of $2 M_{\odot}$. Shown is a snapshot of the flame evolution at 0.9 s after the explosion. It is clearly visible that the propagation of the wrinkled deflagration flame (reddish surface) is inhibited in lateral directions by the rotation and propagates predominantly along the rotation axis. At several location a deflagration-to-detonation transition occurred and detonation flames started to spread (whitish surface). The donut structure of the differentially rotating WD is indicated by the blueish volume rendering of its density.

Yielding a total ^{56}Ni mass of $1.45 M_{\odot}$ our simulation gives rise to a bright explosion which in principle qualifies the model as an explanation of super-luminous SNe Ia. However, the observationally derived ejecta structure of those objects [96] does not match our explosion. This is also reflected by the synthetic observables from our model which do not match the observed spectra of super-luminous SNe Ia (see Fig. 13). In particular absorption features of intermediate-mass elements, such as Si and S, are significantly blue-shifted with respect to the observed

spectra, thus indicating that these elements are located at too large velocities in our model. Moreover, we cannot reproduce the characteristic C features of super-luminous SNe Ia in our model since the detonation burns almost all the fuel.

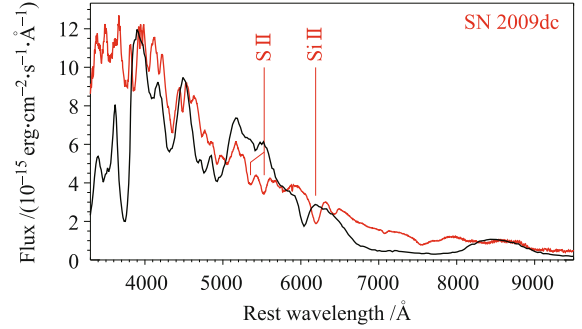


Fig. 13 Synthetic maximum light spectrum of a delayed detonation in a differentially rotating WD of $2 M_{\odot}$. The characteristic absorption features of Si and S are blue-shifted with respect to the observed spectrum of SN 2009dc [61], a proto-typical super-luminous SNe Ia. The binding energy of the WD is not large enough to compensate for the huge energy release due to nuclear burning leading to a too high kinetic energy.

As an alternative explanation for super-luminous SNe Ia Howell *et al.* [90] proposed the merger of two massive CO WDs. However, at least in the violent WD merger scenario [224], this seems to be unlikely. In this model the produced ^{56}Ni mass depends only on the mass of the primary WD. Since exploding CO WDs in the violent merger model usually have masses well below $1.3 M_{\odot}$ [116], this essentially limits the achievable ^{56}Ni mass in a violent merger to $\sim 1 M_{\odot}$. For an alternative explanation of super-luminous SNe Ia in an interaction scenario see Hachinger *et al.* [96].

5 Summary and conclusions

In this article we have reviewed some of the recent work on SNe Ia done by the MPA-Garching group. Most of this work was motivated by the fact that this class of stellar explosions is not as homogeneous as it appeared to be in the past. In fact, new detailed observations of many nearby events as well as results from recent supernova surveys seem to indicate that there is not a single progenitor channel but that several distinctively different channels are more likely.

Therefore we have started a new effort to simulate not only single-degenerate Chandrasekhar-mass explosions but also sub-Chandrasekhar mass models and (violent) double-degenerate mergers, to compute synthetic light curves and spectra from these models, and to compare their predictions with data. Moreover, we have made an attempt to compute rates and delay times of the different progenitor classes from binary-population synthesis

models. The main results of this program were presented in the previous sections.

We have demonstrated that some of the models are able to reproduce light curves and spectra of “normal” SNe Ia amazingly well, given the fact, that these models have almost no tunable (non-physical) parameters. The agreement is not perfect but, given the uncertainties still present in the models (initial conditions, combustion physics, radiative transfer, ...) this is not so surprising. Also, it may be better not to compare an individual supernova with a particular realization of a special group of models but try to reproduce “generic” features of a full class of objects instead. This will become possible in the future once extended grids of models have been computed.

The bad news is that rather different explosion models reproduce the data equally well (or not so well). This “degeneracy” can be understood from the fact that mainly the abundances and distribution of radioactive ^{56}Ni and intermediate-mass nuclei determine the observed properties of thermonuclear supernovae, and they are not too different for delayed-detonation Chandrasekhar-mass models, for sub-Chandrasekhar-mass explosions, or for violent mergers. These classes of models differ mainly in their ejecta masses and the amount of unburnt carbon and oxygen. But since the opacity of C and O is low this has, in general, little effect on the light curves and spectra. In the future, strong arguments in favor of one or the other progenitor channel may come from constraints on the rates and delay times. Our population synthesis models support the double-degenerate scenario, but this is still controversial. Other constraints come from direct observations, such as the presence or absence of circumstellar gas, the non-detection of the progenitor star or its companion, and so on. As it stands, the results of such studies are conflicting, but could best be explained by more than one progenitor channel.

As far as some of the peculiar SNe Ia are concerned models appear to be more conclusive. We have shown that SN 2002cx-like supernovae can be explained well by pure deflagrations of Chandrasekhar-mass WDs that leave behind a bound WD. SN 1991bg-like events, in contrast, can be explained by a violent merger of two WDs of almost equal mass around $0.9 M_{\odot}$. Finally, in our simulations we did not find an explanation of the superluminous SNe Ia. Neither the merger of two massive WDs nor the explosion of a rapidly-rotating super-Chandrasekhar-mass WD can reproduce the high luminosity and rather normal expansion velocity at the same time. Here, one might speculate that not all the luminosity comes from radioactive decay.

and, in particular, to Franco Ciaraldi-Schoolman, Michael Fink, Rüdiger Pakmor, Ivo Seitenzahl, Stuart Sim, and Stefan Taubenberger for many inspiring discussions and their valuable contributions to the work that is presented in this review. This work was supported by the Deutsche Forschungsgemeinschaft via the Transregional Collaborative Research Center TRR 33 and the Excellence Cluster EXC 153. The research of F.K.R. is supported by the Emmy Noether Program (RO 3676/1-1) of the Deutsche Forschungsgemeinschaft and by the ARCHES prize of the German Federal Ministry of Education and Research (BMBF). The simulations were performed at the Jülich supercomputing center (grants PRACE026, PRACE042 and HMU014), the Computing Center Garching of the Max-Planck-Gesellschaft and NCI at the ANU.

References and notes

1. W. D. Arnett, *Astrophys. Space Sci.*, 1969, 5(2): 180
2. K. Nomoto, F. K. Thielemann, and K. Yokoi, *Astrophys. J.*, 1984, 286: 644
3. W. Hillebrandt and J. C. Niemeyer, *Ann. Rev. Astron. Astrophys.*, 2000, 38: 191, arXiv: astro-ph/0006305
4. F. Hoyle and W. A. Fowler, *Astrophys. J.*, 1960, 132: 565
5. P. E. Nugent, M. Sullivan, S. B. Cenko, R. C. Thomas, et al., *Nature*, 2011, 480(7377): 344, arXiv: 1110.6201
6. J. S. Bloom, D. Kasen, K. J. Shen, P. E. Nugent, N. R. Butler, M. L. Graham, D. A. Howell, U. Kolb, S. Holmes, C. Haswell, V. Burwitz, J. Rodriguez, and M. Sullivan, *Astrophys. J.*, 2012, 744: L17, arXiv: 1111.0966
7. S. Rosswog, E. Ramirez-Ruiz, and W. R. Hix, *Astrophys. J.*, 2008, 679: 1385, arXiv: 0712.2513
8. S. Rosswog, D. Kasen, J. Guillochon, and E. Ramirez-Ruiz, *Astrophys. J.*, 2009, 705: L128, arXiv: 0907.3196
9. C. Raskin, F. X. Timmes, E. Scannapieco, S. Diehl, and C. Fryer, *Mon. Not. R. Astron. Soc.*, 2009, 399(1): L156, arXiv: 0907.3915
10. M. M. Phillips, *Astrophys. J.*, 1993, 413: L105
11. A. G. Riess, W. H. Press, and R. P. Kirshner, *Astrophys. J.*, 1996, 473: 88, arXiv: astro-ph/9604143
12. D. Branch, *Ann. Rev. Astron. Astrophys.*, 1998, 36: 17, arXiv: astro-ph/9801065
13. B. P. Schmidt, N. B. Suntzeff, M. M. Phillips, R. A. Schommer, et al., *Astrophys. J.*, 1998, 507: 46, arXiv: astro-ph/9805200
14. A. G. Riess, A. V. Filippenko, P. Challis, A. Clocchiatti, et al., *Astron. J.*, 1998, 116: 1009, arXiv: astro-ph/9805201
15. S. Perlmutter, G. Aldering, G. Goldhaber, R. A. Knop, et al., *Astrophys. J.*, 1999, 517: 565, arXiv: astro-ph/9812133
16. J. L. Tonry, B. P. Schmidt, B. Barris, P. Candia, et al., *Astrophys. J.*, 2003, 594: 1, arXiv: astro-ph/0305008
17. A. G. Riess, L. G. Strolger, J. Tonry, S. Casertano, et al., *Astrophys. J.*, 2004, 607: 665, arXiv: astro-ph/0402512
18. P. Astier, J. Guy, N. Regnault, R. Pain, et al., *Astron. Astrophys.*, 2006, 447: 31, arXiv: astro-ph/0510447
19. A. G. Riess, L. G. Strolger, S. Casertano, H. C. Ferguson, et al., *Astrophys. J.*, 2007, 659: 98, arXiv: astro-ph/0611572

Acknowledgements We are grateful to MPA’s SN Ia group

20. C. Mignone and M. Bartelmann, *Astron. Astrophys.*, 2008, 481: 295, arXiv: 0711.0370
21. S. Benitez-Herrera, *Mon. Not. R. Astron. Soc.*, 2012, 419: 513, arXiv: 1109.0873
22. A. Goobar and B. Leibundgut, *Ann. Rev. Nucl. Part. Sci.*, 2011, 61(1): 251, arXiv: 1102.1431
23. A. V. Filippenko, in: *Thermonuclear Supernovae*, edited by P. Ruiz-Lapuente, R. Canal, and J. Isern, Vol. 486 of NATO ASIC Proc., Dordrecht: Kluwer Academic Publishers, 1997: 1
24. B. Leibundgut, *Astron. Astrophys. Rev.*, 2000, 10: 179, arXiv: astro-ph/0003326
25. B. Leibundgut, *Gen. Relativ. Gravit.*, 2008, 40(2-3): 221, arXiv: 0802.4154
26. A. V. Filippenko, *Ann. Rev. Astron. Astrophys.*, 1997, 35(1): 309
27. D. Branch, L. C. Dang, and E. Baron, *Publications of the Astronomical Society of the Pacific*, 2009, 121: 238, arXiv: 0902.0745
28. W. P. S. Meikle, R. J. Cumming, T. R. Geballe, J. R. Lewis, et al., *Mon. Not. R. Astron. Soc.*, 1996, 281: 263
29. W. P. S. Meikle, *Mon. Not. R. Astron. Soc.*, 2000, 314: 782, arXiv: astro-ph/9912123
30. B. Leibundgut and N. B. Suntzeff, in: *Supernovae and Gamma-Ray Bursters*, edited by K. Weiler, Vol. 598 of *Lecture Notes in Physics*, Berlin: Springer-Verlag, 2003: 77, arXiv: astro-ph/0304112
31. J. C. Wheeler and R. P. Harkness, *Rep. Prog. Phys.*, 1990, 53(12): 1467
32. D. Branch, A. Fisher, and P. Nugent, *Astron. J.*, 1993, 106: 2383
33. W. Li, J. Leaman, R. Chornock, A. V. Filippenko, D. Poznanski, M. Ganeshalingam, X. Wang, M. Modjaz, S. Jha, R. J. Foley, and N. Smith, *Mon. Not. R. Astron. Soc.*, 2011, 412(3): 1441, arXiv: 1006.4612
34. R. Harkness, in: *European Southern Observatory Conference and Workshop Proceedings*, edited by I. J. Danziger and K. Kjaer, Vol. 37 of *European Southern Observatory Conference and Workshop Proceedings*, 1991: 447
35. M. J. Kuchner, R. P. Kirshner, P. A. Pinto, and B. Leibundgut, *Astrophys. J.*, 1994, 426: L89
36. J. W. Truran, W. D. Arnett, and A. G. W. Cameron, *Can. J. Phys.*, 1967, 45(7): 2315
37. S. A. Colgate and C. McKee, *Astrophys. J.*, 1969, 157: 623
38. F. Patat, S. Benetti, E. Cappellaro, I. J. Danziger, M. della Valle, P. A. Mazzali, and M. Turatto, *Mon. Not. R. Astron. Soc.*, 1996, 278: 111
39. M. Stehle, P. A. Mazzali, S. Benetti, and W. Hillebrandt, *Mon. Not. R. Astron. Soc.*, 360, 1231 (2005), arXiv: astro-ph/0409342
40. G. Garavini, S. Nobili, S. Taubenberger, A. Pastorello, et al., *Astron. Astrophys.*, 2007, 471: 527, arXiv: astro-ph/0702569
41. A. G. Riess, A. V. Filippenko, W. Li, R. R. Treffers, et al., *Astron. J.*, 1999, 118: 2675, arXiv: astro-ph/9907037
42. M. Strovink, *Astrophys. J.*, 2007, 671: 1084, arXiv: 0705.0726
43. A. Conley, D. A. Howell, A. Howes, M. Sullivan, et al., *Astron. J.*, 2006, 132: 1707, arXiv: astro-ph/0607363
44. B. T. Hayden, P. M. Garnavich, R. Kessler, J. A. Frieman, et al., *Astrophys. J.*, 2010, 712: 350, arXiv: 1001.3428
45. M. Hamuy, M. M. Phillips, N. B. Suntzeff, R. A. Schommer, J. Maza, and R. Aviles, *Astron. J.*, 1996, 112: 2391, arXiv: astro-ph/9609059
46. M. Stritzinger, B. Leibundgut, S. Walch, and G. Contardo, *Astron. Astrophys.*, 2006, 450: 241, arXiv: astro-ph/0506415
47. D. C. Leonard, *Astrophys. J.*, 2007, 670: 1275, arXiv: 0710.3166
48. P. A. Mazzali and L. B. Lucy, *Mon. Not. R. Astron. Soc.*, 1998, 295(2): 428
49. M. Hamuy, M. M. Phillips, N. B. Suntzeff, J. Maza, et al., *Nature*, 2003, 424: 651, arXiv: astro-ph/0306270
50. B. Dilday, D. A. Howell, S. B. Cenko, J. M. Silverman, et al., *Science*, 2012, 337(6097): 942, arXiv: 1207.1306
51. L. Chomiuk, A. M. Soderberg, R. Chevalier, C. Badenes, and C. Fransson, in: *American Astronomical Society Meeting Abstracts 217*, Vol. 43 of *Bulletin of the American Astronomical Society*, 2011: 304.05
52. L. Chomiuk, A. M. Soderberg, M. Moe, R. A. Chevalier, M. P. Rupen, C. Badenes, R. Margutti, C. Fransson, W. F. Fong, and J. A. Dittmann, *Astrophys. J.*, 2012, 750: 164, arXiv: 1201.0994
53. A. Horeh, S. R. Kulkarni, D. B. Fox, J. Carpenter, et al., *Astrophys. J.*, 2012, 746: 21, arXiv: 1109.2912
54. I. P. Pskovskii, *Sov. Astron.*, 1977, 21: 675
55. D. Branch, *Astrophys. J.*, 1981, 248: 1076
56. P. A. Mazzali, F. K. Röpkke, S. Benetti, and W. Hillebrandt, *Science*, 2007, 315: 825, arXiv: astro-ph/0702351
57. M. Hicken, P. Challis, S. Jha, R. P. Kirshner, et al., *Astrophys. J.*, 2009, 700: 331, arXiv: 0901.4787
58. M. M. Phillips, P. Lira, N. B. Suntzeff, R. A. Schommer, M. Hamuy, and J. Maza, *Astron. J.*, 1999, 118: 1766, arXiv: astro-ph/9907052
59. S. Taubenberger, S. Hachinger, G. Pignata, P. A. Mazzali, et al., *Mon. Not. R. Astron. Soc.*, 2008, 385: 75, arXiv: 0711.4548
60. M. M. Phillips, W. Li, J. A. Frieman, S. I. Blinnikov, et al., *Publications of the Astronomical Society of the Pacific*, 2007, 119: 360, arXiv: astro-ph/0611295
61. S. Taubenberger, S. Benetti, M. Childress, R. Pakmor, et al., *Mon. Not. R. Astron. Soc.*, 2011, 412(4): 2735, arXiv: 1011.5665
62. S. Perlmutter, S. Gabi, G. Goldhaber, A. Goobar, et al., *Astrophys. J.*, 1997, 483: 565, arXiv: astro-ph/9608192
63. M. Kowalski, D. Rubin, G. Aldering, R. J. Agostinho, et al., *Astrophys. J.*, 2008, 686: 749, arXiv: 0804.4142

64. R. Amanullah, C. Lidman, D. Rubin, G. Aldering, et al., arXiv: 1004.1711, 2010
65. H. Lampeitl, R. C. Nichol, H. J. Seo, T. Giannantonio, et al., *Mon. Not. R. Astron. Soc.*, 2010, 401(4): 2331
66. J. Guy, M. Sullivan, A. Conley, N. Regnault, et al., *Astron. Astrophys.*, 2010, 523: A7, arXiv: 1010.4743
67. A. Conley, J. Guy, M. Sullivan, N. Regnault, et al., *Astrophys. J. Suppl.*, 2011, 192: 1, arXiv: 1104.1443
68. N. Suzuki, D. Rubin, C. Lidman, G. Aldering, et al., *Astrophys. J.*, 2012, 746: 85, arXiv: 1105.3470
69. A. V. Filippenko, M. W. Richmond, T. Matheson, J. C. Shields, E. M. Burbidge, R. D. Cohen, M. Dickinson, M. A. Malkan, B. Nelson, J. Pietz, D. Schlegel, P. Schmeer, H. Spinrad, C. C. Steidel, H. D. Tran, and W. Wren, *Astrophys. J.*, 1992, 384: L15
70. B. Leibundgut, R. P. Kirshner, M. M. Phillips, L. A. Wells, et al., *Astron. J.*, 1993, 105: 301
71. M. Hamuy, M. M. Phillips, J. Maza, N. B. Suntzeff, et al., *Astron. J.*, 1994, 108: 2226
72. M. Turatto, S. Benetti, E. Cappellaro, I. J. Danziger, M. Della Valle, C. Gouffes, P. A. Mazzali, and F. Patat, *Mon. Not. R. Astron. Soc.*, 1996, 283: 1 arXiv: astro-ph/9605178
73. P. M. Garnavich, A. Z. Bonanos, K. Krisciunas, S. Jha, et al., *Astrophys. J.*, 2004, 613: 1120, arXiv: astro-ph/0105490
74. P. A. Mazzali, N. Chugai, M. Turatto, L. B. Lucy, I. J. Danziger, E. Cappellaro, M. della Valle, and S. Benetti, *Mon. Not. R. Astron. Soc.*, 1997, 284: 151
75. W. Li, A. V. Filippenko, R. Chornock, E. Berger, et al., *Publications of the Astronomical Society of the Pacific*, 2003, 115: 453, arXiv: astro-ph/0301428
76. S. Jha, R. P. Kirshner, P. Challis, P. M. Garnavich, et al., *Astron. J.*, 2006, 131: 527, arXiv: astro-ph/0509234
77. W. D. Arnett, *Astrophys. J.*, 1982, 253: 785
78. D. K. Sahu, M. Tanaka, G. C. Anupama, K. S. Kawabata, K. Maeda, N. Tominaga, K. Nomoto, P. A. Mazzali, and T. P. Prabhu, *Astrophys. J.*, 2008, 680: 580, arXiv: 0710.3636
79. R. J. Foley, A. Rest, M. Stritzinger, G. Pignata, J. P. Anderson, M. Hamuy, N. I. Morrell, M. M. Phillips, and F. Salgado, *Astron. J.*, 2010, 140: 1321, arXiv: 1008.0635
80. G. Narayan, R. J. Foley, E. Berger, M. T. Botticella, R. Chornock, M. E. Huber, A. Rest, D. Scolnic, S. Smartt, S. Valenti, et al., *Astrophys. J.*, 2011, 731: L11, arXiv: 1008.4353
81. H. B. Perets, A. Gal-Yam, P. A. Mazzali, D. Arnett, et al., *Nature*, 2010, 465(7296): 322
82. K. S. Kawabata, K. Maeda, K. Nomoto, S. Taubenberger, M. Tanaka, J. Deng, E. Pian, T. Hattori, and K. Itagaki, *Nature*, 2010, 465(7296): 326
83. R. Waldman, D. Sauer, E. Livne, H. Perets, A. Glasner, P. Mazzali, J. W. Truran, and A. Gal-Yam, *Astrophys. J.*, 2011, 738: 21, arXiv: 1009.3829
84. K. Maeda, T. Moriya, K. Kawabata, M. Tanaka, N. Tominaga, and K. Nomoto, *Mem. Soc. Astron. Ital.*, 2012, 83: 264
85. M. M. Kasliwal, S. R. Kulkarni, A. Gal-Yam, P. E. Nugent, et al., *Astrophys. J.*, 2012, 755: 161, arXiv: 1111.6109
86. M. M. Phillips, L. A. Wells, N. B. Suntzeff, M. Hamuy, B. Leibundgut, R. P. Kirshner, and C. B. Foltz, *Astron. J.*, 1992, 103: 1632
87. D. J. Jeffery, B. Leibundgut, R. P. Kirshner, S. Benetti, D. Branch, and G. Sonneborn, *Astrophys. J.*, 1992, 397: 304
88. P. Ruiz-Lapuente, E. Cappellaro, M. Turatto, C. Gouffes, I. J. Danziger, M. della Valle, and L. B. Lucy, *Astrophys. J.*, 1992, 387: L33
89. J. Spyromilio, W. P. S. Meikle, D. A. Allen, and J. R. Graham, *Mon. Not. R. Astron. Soc.*, 1992, 258: 53P
90. D. A. Howell, M. Sullivan, P. E. Nugent, R. S. Ellis, et al., *Nature*, 2006, 443: 308, arXiv: astro-ph/0609616
91. M. Hicken, P. M. Garnavich, J. L. Prieto, S. Blondin, D. L. DePoy, R. P. Kirshner, and J. Parrent, *Astrophys. J.*, 2007, 669: L17, arXiv: 0709.1501
92. M. Yamanaka, K. S. Kawabata, K. Kinugasa, M. Tanaka, et al., *Astrophys. J.*, 2009, 707: L118, arXiv: 0908.2059
93. M. Tanaka, K. S. Kawabata, M. Yamanaka, K. Maeda, et al., *Astrophys. J.*, 2010, 714: 1209, arXiv: 0908.2057
94. J. M. Silverman, M. Ganeshalingam, W. Li, A. V. Filippenko, A. A. Miller, and D. Poznanski, *Mon. Not. R. Astron. Soc.*, 2011, 410(1): 585, arXiv: 1003.2417
95. Y. Kamiya, M. Tanaka, K. Nomoto, S. I. Blinnikov, E. I. Sorokina, and T. Suzuki, *Astrophys. J.*, 2012, 756: 191, arXiv: 1207.4648
96. S. Hachinger, P. A. Mazzali, S. Taubenberger, M. Fink, R. Pakmor, W. Hillebrandt, and I. R. Seitenzahl, arXiv: 1209.1339, 2012
97. A. Fisher, D. Branch, K. Hatano, and E. Baron, *Mon. Not. R. Astron. Soc.*, 1999, 304(1): 67, arXiv: astro-ph/9807032
98. M. Sullivan, D. Le Borgne, C. J. Pritchett, A. Hodsman, et al., *Astrophys. J.*, 2006, 648: 868, arXiv: astro-ph/0605455
99. D. A. Howell, M. Sullivan, E. F. Brown, A. Conley, et al., *Astrophys. J.*, 2009, 691: 661, arXiv: 0810.0031
100. M. Hicken, W. M. Wood-Vasey, S. Blondin, P. Challis, S. Jha, P. L. Kelly, A. Rest, and R. P. Kirshner, *Astrophys. J.*, 2009, 700: 1097, arXiv: 0901.4804
101. P. L. Kelly, M. Hicken, D. L. Burke, K. S. Mandel, and R. P. Kirshner, *Astrophys. J.*, 2010, 715: 743, arXiv: 0912.0929
102. M. Sullivan, A. Conley, D. A. Howell, J. D. Neill, et al., *Mon. Not. R. Astron. Soc.*, 2010, 406: 782, arXiv: 1003.5119
103. D. Branch, W. Romanishin, and E. Baron, *Astrophys. J.*, 1996, 465: 73, arXiv: astro-ph/9510071
104. J. S. Gallagher, P. M. Garnavich, P. Berlind, P. Challis, S. Jha, and R. P. Kirshner, *Astrophys. J.*, 2005, 634: 210, arXiv: astro-ph/0508180
105. R. J. Foley, P. J. Challis, A. V. Filippenko, M. Ganeshalingam, et al., *Astrophys. J.*, 2012, 744: 38, arXiv: 1109.0987
106. S. Blondin, L. Dessart, B. Leibundgut, D. Branch, et al., *Astron. J.*, 2006, 131: 1648, arXiv: astro-ph/0510089
107. T. J. Bronder, I. M. Hook, P. Astier, D. Balam, et al., *Astron. Astrophys.*, 2008, 477: 717, arXiv: 0709.0859

108. F. Mannucci, M. Della Valle, N. Panagia, E. Cappellaro, G. Cresci, R. Maiolino, A. Petrosian, and M. Turatto, *Astron. Astrophys.*, 2005, 433: 807, arXiv: astro-ph/0411450
109. W. Li, J. S. Bloom, P. Podsiadlowski, A. A. Miller, et al., *Nature*, 2011, 480(7377): 348, arXiv: 1109.1593
110. O. Graur and D. Maoz, arXiv: 1209.0008, 2012
111. E. Cappellaro, R. Evans, and M. Turatto, *Astron. Astrophys.*, 1999, 351: 459, arXiv: astro-ph/9904225
112. K. Perrett, M. Sullivan, A. Conley, S. González-Gaitán, et al., *Astron. J.*, 2012, 144: 59, arXiv: 1206.0665
113. L. Wang, P. Hoeich, and J. C. Wheeler, *Astrophys. J.*, 1997, 483(1): L29
114. B. Wang and Z. Han, *New Astron. Rev.*, 2012, 56: 122, arXiv: 1204.1155
115. I. Iben, Jr. and A. V. Tutukov, *Astrophys. J. Suppl.*, 1984, 54: 335
116. A. J. Ruiter, S. A. Sim, R. Pakmor, M. Kromer, I. R. Seitenzahl, K. Belczynski, M. Fink, M. Herzog, W. Hillebrandt, F. K. Roepke, S. Taubenberger, *Mon. Not. R. Astron. Soc.*, 2012: 362, arXiv: 1209.0645
117. K. Belczynski, V. Kalogera, F. A. Rasio, R. E. Taam, A. Zezas, T. Bulik, T. J. Maccarone, and N. Ivanova, *Astrophys. J. Suppl.*, 2008, 174: 223, arXiv: astro-ph/0511811
118. G. Nelemans, S. Toonen, and M. Bours, in: *Binary Paths to Type Ia Supernova Explosions*, arXiv: 1204.2960, 2012
119. N. Mennekens, D. Vanbeveren, J. P. De Greve, and E. De Donder, *Astron. Astrophys.*, 2010, 515: A89, arXiv: 1003.2491
120. Z. Han and P. Podsiadlowski, *Mon. Not. R. Astron. Soc.*, 2004, 350(4): 1301, arXiv: astro-ph/0309618
121. S. F. Portegies Zwart, L. R. Yungelson, and G. Nelemans, in: *The Formation of Binary Stars*, edited by H. Zinnecker and R. Mathieu, vol. 200 of *IAU Symposium*, 2001: 505, arXiv: astro-ph/0008033
122. D. Maoz and F. Mannucci, *Publications of the Astronomical Society of Australia*, 2012, 29: 447, arXiv: 1111.4492
123. J. Whelan and I. J. Iben, *Astrophys. J.*, 1973, 186: 1007
124. I. Hachisu, M. Kato, and G. J. M. Luna, *Astrophys. J.*, 2007, 659: L153, arXiv: astro-ph/0703185
125. K. Nomoto, H. Saio, M. Kato, and I. Hachisu, *Astrophys. J.*, 2007, 663: 1269, arXiv: astro-ph/0603351
126. A. J. Ruiter, K. Belczynski, and C. Fryer, *Astrophys. J.*, 2009, 699: 2026, arXiv: 0904.3108
127. B. Paczynski, in: *Structure and Evolution of Close Binary Systems*, edited by P. Eggleton, S. Mitton, and J. Whelan, Vol. 73 of *IAU Symposium*, 1976: 75
128. J. E. Solheim and L. R. Yungelson, in: *14th European Workshop on White Dwarfs*, edited by D. Koester and S. Moehler, Vol. 334 of *Astronomical Society of the Pacific Conference Series*, 2005: 387, arXiv: astro-ph/0411053
129. K. Iben, A. Nomoto, Tornambe, and A. V. Tutukov, *Astrophys. J.*, 1987, 317: 717
130. B. Wang, X. Chen, X. Meng, and Z. Han, *Astrophys. J.*, 2009, 701: 1540, arXiv: 0906.4148
131. A. J. Ruiter, K. Belczynski, S. A. Sim, W. Hillebrandt, C. L. Fryer, M. Fink, and M. Kromer, *Mon. Not. R. Astron. Soc.*, 2011, 417(1): 408, arXiv: 1011.1407
132. R. E. Taam, *Astrophys. J.*, 1980, 242: 749
133. K. J. Shen, D. Kasen, N. N. Weinberg, L. Bildsten, and E. Scannapieco, *Astrophys. J.*, 2010, 715: 767, arXiv: 1002.2258
134. A. Tutukov and L. Yungelson, *Mon. Not. R. Astron. Soc.*, 1996, 280: 1035
135. L. Yungelson, M. Livio, A. Tutukov, and S. J. Kenyon, *Astrophys. J.*, 1995, 447: 656
136. I. Iben, Jr. and A. V. Tutukov, *Astrophys. J. Suppl.*, 1996, 105: 145
137. L. R. Yungelson, and M. Livio, *Astrophys. J.*, 2000, 528: 108, arXiv: astro-ph/9907359
138. I. Iben, Jr. and A. V. Tutukov, *Astrophys. J.*, 1991, 370: 615
139. R. F. Webbink, *Astrophys. J.*, 1984, 277: 355
140. L. R. Yungelson, M. Livio, A. V. Tutukov, and R. A. Saffer, *Astrophys. J.*, 1994, 420: 336
141. S. Toonen, G. Nelemans, and S. Portegies Zwart, *Astron. Astrophys.*, 2012, 546: A70, arXiv: 1208.6446
142. D. Maoz, K. Sharon, and A. Gal-Yam, *Astrophys. J.*, 2010, 722: 1879, arXiv: 1006.3576
143. A. J. Ruiter, K. Belczynski, M. Benacquista, S. L. Larson, and G. Williams, *Astrophys. J.*, 2010, 717: 1006, arXiv: 0705.3272
144. H. Saio and K. Nomoto, *Astron. Astrophys.*, 1985, 150: L21
145. S. Miyaji, K. Nomoto, K. Yokoi, and D. Sugimoto, *Publications of the Astronomical Society of Japan*, 1980, 32: 303
146. M. H. van Kerkwijk, P. Chang, and S. Justham, *Astrophys. J.*, 2010, 722: L157, arXiv: 1006.4391
147. C. Badenes and D. Maoz, *Astrophys. J.*, 2012, 749: L11, arXiv: 1202.5472
148. W. M. Sparks and T. P. Stecher, *Astrophys. J.*, 1974, 188: 149
149. M. Livio and A. G. Riess, *Astrophys. J.*, 2003, 594: L93, arXiv: astro-ph/0308018
150. M. Ilkov and N. Soker, *Mon. Not. R. Astron. Soc.*, 2012, 419: 1695, arXiv: 1106.2027
151. F. Förster, C. Wolf, P. Podsiadlowski, and Z. Han, *Mon. Not. R. Astron. Soc.*, 2006, 368(4): 1893, arXiv: astro-ph/0601454
152. T. Totani, T. Morokuma, T. Oda, M. Doi, and N. Yasuda, *Publications of the Astronomical Society of Japan*, 2008, 60: 1327, arXiv: 0804.0909
153. D. Maoz, F. Mannucci, and T. D. Brandt, *Mon. Not. R. Astron. Soc.*, 2012, 426(4): 3282
154. P. C. Peters, *Phys. Rev.*, 1964, 136(4B): B1224. Available at: <http://link.aps.org/doi/10.1103/PhysRev.136.B1224>
155. T. A. Thompson, *Astrophys. J.*, 2011, 741: 82, arXiv: 1011.4322
156. M. Zingale, A. S. Almgren, J. B. Bell, A. Nonaka, and S. E. Woosley, *Astrophys. J.*, 2009, 704: 196, arXiv: 0908.2668

157. A. Nonaka, A. J. Aspden, M. Zingale, A. S. Almgren, J. B. Bell, and S. E. Woosley, *Astrophys. J.*, 2012, 745: 73, arXiv: 1111.3086
158. A. Khokhlov, *Astrophys. J.*, 1993, 419: L77
159. A. M. Khokhlov, *Astrophys. J.*, 1995, 449: 695
160. M. Reinecke, W. Hillebrandt, J. C. Niemeyer, R. Klein, and A. Gröbl, *Astron. Astrophys.*, 1999, 347: 724, arXiv: astro-ph/9812119
161. M. Reinecke, W. Hillebrandt, and J. C. Niemeyer, *Astron. Astrophys.*, 1999, 347: 739, arXiv: astro-ph/9812120
162. F. X. Timmes and S. E. Woosley, *Astrophys. J.*, 1992, 396: 649
163. G. J. Sharpe, *Mon. Not. R. Astron. Soc.*, 1999, 310(4): 1039
164. C. Travaglio, W. Hillebrandt, M. Reinecke, and F. K. Thielemann, *Astron. Astrophys.*, 2004, 425: 1029, arXiv: astro-ph/0406281
165. I. R. Seitenzahl, F. K. Röpke, M. Fink, and R. Pakmor, *Mon. Not. R. Astron. Soc.*, 2010, 407: 2297, arXiv: 1005.5071
166. F. K. Röpke, *Astron. Astrophys.*, 2005, 432: 969, arXiv: astro-ph/0408296
167. F. K. Röpke and W. Hillebrandt, *Astron. Astrophys.*, 2005, 429: L29, arXiv: astro-ph/0411667
168. F. K. Röpke, W. Hillebrandt, J. C. Niemeyer, and S. E. Woosley, *Astron. Astrophys.*, 2006, 448: 1, arXiv: astro-ph/0510474
169. P. A. Mazzali and L. B. Lucy, *Astron. Astrophys.*, 1993, 279: 447, <http://adsabs.harvard.edu/abs/1993A&A...279.447M>
170. P. A. Pinto and R. G. Eastman, *Astrophys. J.*, 2000, 530(2): 757
171. D. Branch, R. Buta, S. W. Falk, M. L. McCall, A. Uomoto, J. C. Wheeler, B. J. Wills, and P. G. Sutherland, *Astrophys. J.*, 1982, 252: L61
172. D. Branch, C. H. Lacy, M. L. McCall, P. G. Sutherland, A. Uomoto, J. C. Wheeler, and B. J. Wills, *Astrophys. J.*, 1983, 270: 123
173. L. B. Lucy, *Astron. Astrophys.*, 1999, 345: 211, <http://adsabs.harvard.edu/abs/1999A&A...345.211L>
174. D. Kasen, R. C. Thomas, and P. Nugent, *Astrophys. J.*, 2006, 651: 366, arXiv: astro-ph/0606111
175. L. B. Lucy, *Astron. Astrophys.*, 2002, 384: 725, arXiv: astro-ph/0107377
176. L. B. Lucy, *Astron. Astrophys.*, 2003, 403: 261, arXiv: astro-ph/0303202
177. L. B. Lucy, *Astron. Astrophys.*, 2005, 429: 19, arXiv: astro-ph/0409249
178. M. Kromer and S. A. Sim, *Mon. Not. R. Astron. Soc.*, 2009, 398(4): 1809, arXiv: 0906.3152
179. S. A. Sim, *Mon. Not. R. Astron. Soc.*, 2007, 375: 154, arXiv: astro-ph/0611677
180. S. A. Sim and P. A. Mazzali, *Mon. Not. R. Astron. Soc.*, 2008, 385(4): 1681, arXiv: 0710.3313
181. R. Kurucz and B. Bell, Cambridge, MA: Smithsonian Astrophysical Observatory, 1995, <http://kurucz.harvard.edu/cdroms.html>
182. V. V. Sobolev, *Sov. Astron.*, 1957, 1: 678
183. M. Zingale, S. E. Woosley, C. A. Rendleman, M. S. Day, and J. B. Bell, *Astrophys. J.*, 2005, 632: 1021, arXiv: astro-ph/0501655
184. F. Ciaraldi-Schoolmann, W. Schmidt, J. C. Niemeyer, F. K. Röpke, and W. Hillebrandt, *Astrophys. J.*, 2009, 696: 1491, arXiv: 0901.4254
185. J. C. Niemeyer and W. Hillebrandt, *Astrophys. J.*, 1995, 452: 769
186. W. Schmidt, J. C. Niemeyer, W. Hillebrandt, and F. K. Röpke, *Astron. Astrophys.*, 2006, 450: 283, arXiv: astro-ph/0601500
187. G. Damköhler, *Z. f. Elektroch.*, 1940, 46: 601
188. F. K. Röpke and W. Schmidt, in *Interdisciplinary Aspects of Turbulence*, edited by W. Hillebrandt and F. Kupka, Lecture Notes in Physics, Berlin: Springer-Verlag, 2009: 255
189. P. Höflich and J. Stein, *Astrophys. J.*, 2002, 568: 779, arXiv: astro-ph/0104226
190. M. Kuhlen, S. E. Woosley, and G. A. Glatzmaier, *Astrophys. J.*, 2006, 640: 407, arXiv: astro-ph/0509367
191. F. K. Röpke, W. Hillebrandt, W. Schmidt, J. C. Niemeyer, S. I. Blinnikov, and P. A. Mazzali, *Astrophys. J.*, 2007, 668: 1132, arXiv: 0707.1024
192. F. K. Röpke, M. Kromer, I. R. Seitenzahl, R. Pakmor, et al., *Astrophys. J.*, 2012, 750: L19, arXiv: 1203.4839
193. I. R. Seitenzahl, F. Ciaraldi-Schoolmann, F. K. Röpke, M. Fink, W. Hillebrandt, M. Kromer, R. Pakmor, A. J. Ruiter, S. A. Sim, and S. Taubenberger, *Mon. Not. R. Astron. Soc.*, 2012: 315 arXiv: 1211.3015
194. A. M. Khokhlov, *Astron. Astrophys.*, 1991, 245: 114
195. F. K. Röpke and J. C. Niemeyer, *Astron. Astrophys.*, 2007, 464: 683, arXiv: astro-ph/0703378
196. F. K. Röpke, M. Gieseler, M. Reinecke, C. Travaglio, and W. Hillebrandt, *Astron. Astrophys.*, 2006, 453: 203, arXiv: astro-ph/0506107
197. B. K. Krueger, A. P. Jackson, D. M. Townsley, A. C. Calder, E. F. Brown, and F. X. Timmes, *Astrophys. J.*, 2010, 719: L5, arXiv: 1007.0910
198. A. P. Jackson, A. C. Calder, D. M. Townsley, D. A. Chamulak, E. F. Brown, and F. X. Timmes, *Astrophys. J.*, 2010, 720: 99, arXiv: 1007.1138
199. I. R. Seitenzahl, F. Ciaraldi-Schoolmann, and F. K. Röpke, *Mon. Not. R. Astron. Soc.*, 2011, 414: 2709, arXiv: 1012.4929
200. W. Schmidt and J. C. Niemeyer, *Astron. Astrophys.*, 2006, 446: 627, arXiv: astro-ph/0510427
201. F. K. Röpke, S. E. Woosley, and W. Hillebrandt, *Astrophys. J.*, 2007, 660: 1344, arXiv: astro-ph/0609088
202. R. T. IV Jordan, D. M. Fisher, A. C. Townsley, C. Calder, S. Graziani, D. Q. Asida, D. Q. Lamb, and J. W. Truran, *Astrophys. J.*, 2008, 681(2): 1448
203. D. Kasen, F. K. Röpke, and S. E. Woosley, *Nature*, 2009, 460(7257): 869, arXiv: 0907.0708
204. S. Blondin and D. Kasen, *Mon. Not. R. Astron. Soc.*, 2011, 417: 1280, arXiv: 1107.0009

205. M. Kromer, S. A. Sim, and M. Fink, F. K. Röpke, I. R. Seitenzahl, and W. Hillebrandt, *Astrophys. J.*, 2010, 719: 1067, arXiv: 1006.4489
206. R. Pakmor, M. Kromer, S. Taubenberger, and S. A. Sim, F. K. Röpke, and W. Hillebrandt, *Astrophys. J.*, 2012, 747: L10, arXiv: 1201.5123
207. S. A. Sim, F. K. Röpke, W. Hillebrandt, M. Kromer, R. Pakmor, M. Fink, A. J. Ruiter, and I. R. Seitenzahl, *Astrophys. J.*, 2010, 714: L52, arXiv: 1003.2917
208. T. Shigeyama, K. Nomoto, H. Yamaoka, and F. Thielemann, *Astrophys. J.*, 1992, 386: L13
209. S. E. Woosley, and T. A. Weaver, in *Les Houches Session LIV: Supernovae*, edited by S. A. Bludman, R. Mochkovitch, and J. Zinn-Justin, Amsterdam: North-Holland, 1994: 63
210. E. Livne and D. Arnett, *Astrophys. J.*, 1995, 452: 62
211. W. Benz, in: *Thermonuclear Supernovae*, edited by P. Ruiz-Lapuente, R. Canal, and J. Isern, Vol. 486 of NATOASIC Proc., Dordrecht: Kluwer Academic Publishers, 1997: 457
212. E. Livne, in: *Thermonuclear Supernovae*, edited by P. Ruiz-Lapuente, R. Canal, and J. Isern, Vol. 486 of NATOASIC Proc., Dordrecht: Kluwer Academic Publishers, 1997: 425
213. D. García-Senz, E. Bravo, and S. E. Woosley, *Astron. Astrophys.*, 1999, 349: 177
214. J. Guillochon, M. Dan, E. Ramirez-Ruiz, and S. Rosswog, *Astrophys. J.*, 2010, 709: L64, arXiv: 0911.0416
215. P. Höflich and A. Khokhlov, *Astrophys. J.*, 1996, 457: 500, arXiv: astro-ph/9602025
216. P. Höflich, A. Khokhlov, J. C. Wheeler, M. M. Phillips, N. B. Suntzeff, and M. Hamuy, *Astrophys. J.*, 1996, 472: L81, arXiv: astro-ph/9609070
217. P. Nugent, E. Baron, D. Branch, A. Fisher, and P. H. Hauschildt, *Astrophys. J.*, 1997, 485: 812, arXiv: astro-ph/9612044
218. S. E. Woosley and D. Kasen, *Astrophys. J.*, 2011, 734: 38, arXiv: 1010.5292
219. M. Fink, F. K. Röpke, W. Hillebrandt, I. R. Seitenzahl, S. A. Sim, and M. Kromer, *Astron. Astrophys.*, 2010, 514: A53, arXiv: 1002.2173
220. L. Bildsten, K. J. Shen, N. N. Weinberg, and G. Nelemans, *Astrophys. J.*, 2007, 662: L95, arXiv: astro-ph/0703578
221. K. J. Shen and L. Bildsten, *Astrophys. J.*, 2009, 699: 1365, arXiv: 0903.0654
222. M. Fink, W. Hillebrandt, and F. K. Röpke, *Astron. Astrophys.*, 2007, 476: 1133, arXiv: 0710.5486
223. D. M. Townsley, K. Moore, and L. Bildsten, *Astrophys. J.*, 2012, 755: 4, arXiv: 1205.6517
224. R. Pakmor, M. Kromer, F. K. Röpke, S. A. Sim, A. J. Ruiter, and W. Hillebrandt, *Nature*, 2010, 463(7277): 61, arXiv: 0911.0926
225. H. Saio and K. Nomoto, *Astrophys. J.*, 1998, 500: 388, arXiv: astro-ph/9801084
226. V. Springel, *Mon. Not. R. Astron. Soc.*, 2005, 364: 1105, arXiv: astro-ph/0505010
227. R. Pakmor, P. Edelmann, F. K. Röpke, and W. Hillebrandt, *Mon. Not. R. Astron. Soc.*, 2012, 424: 2222, arXiv: 1205.5806
228. F. K. Röpke, *Astrophys. J.*, 2007, 668: 1103, arXiv: 0709.4095
229. S. E. Woosley, *Astrophys. J.*, 2007, 668: 1109, arXiv: 0709.4237
230. S. E. Woosley, A. R. Kerstein, V. Sankaran, A. J. Aspden, and F. K. Röpke, *Astrophys. J.*, 2009, 704: 255, arXiv: 0811.3610
231. A. Y. Poludnenko, T. A. Gardiner, and E. S. Oran, arXiv: 1106.3696, 2011
232. R. Pakmor, S. Hachinger, F. K. Röpke, and W. Hillebrandt, *Astron. Astrophys.*, 2011, 528: A117+, arXiv: 1102.1354
233. E. J. Lentz, E. Baron, D. Branch, P. H. Hauschildt, and P. E. Nugent, *Astrophys. J.*, 2000, 530: 966, arXiv: astro-ph/9906016
234. G. H. Marion, P. Höflich, W. D. Vacca, and J. C. Wheeler, *Astrophys. J.*, 2003, 591: 316, arXiv: astro-ph/0306470
235. C. Kozma, C. Fransson, W. Hillebrandt, C. Travaglio, J. Sollerman, and M. Reinecke, F. K. Röpke, and J. Spyromilio, *Astron. Astrophys.*, 2005, 437: 983, arXiv: astro-ph/0504317
236. D. Kasen, P. Nugent, L. Wang, D. A. Howell, J. C. Wheeler, P. Höflich, D. Baade, E. Baron, and P. H. Hauschildt, *Astrophys. J.*, 2003, 593: 788, arXiv: astro-ph/0301312
237. L. Wang and J. C. Wheeler, *Ann. Rev. Astron. Astrophys.*, 2008, 46: 433, arXiv: 0811.1054
238. J. Gómez-Gomar, J. Isern, and P. Jean, *Mon. Not. R. Astron. Soc.*, 1998, 295(1): 1, arXiv: astro-ph/9709048
239. K. Maeda, Y. Terada, D. Kasen, F. K. Röpke, et al., *Astrophys. J.*, 2012, 760: 54, arXiv: 1208.2094
240. J. Liu, R. Di Stefano, T. Wang, and M. Moe, *Astrophys. J.*, 749, 141 (2012), arXiv: 1110.2506
241. P. J. Brown, K. S. Dawson, M. de Pasquale, C. Gronwall, et al., *Astrophys. J.*, 2012, 753: 22, arXiv: 1110.2538
242. E. Marietta, A. Burrows, and B. Fryxell, *Astrophys. J. Suppl.*, 2000, 128: 615, arXiv: astro-ph/9908116
243. R. Pakmor, F. K. Röpke, A. Weiss, and W. Hillebrandt, *Astron. Astrophys.*, 2008, 489: 943, arXiv: 0807.3331
244. K. C. Pan, P. M. Ricker, and R. E. Taam, *Astrophys. J.*, 2012, 750: 151, arXiv: 1203.1932
245. Z. W. Liu, R. Pakmor, F. K. Röpke, P. Edelmann, B. Wang, M. Kromer, W. Hillebrandt, and Z. W. Han, *Astron. Astrophys.*, 2012, 548: A2, arXiv: 1209.4458
246. P. Ruiz-Lapuente, F. Comeron, J. Méndez, R. Canal, S. J. Smartt, A. V. Filippenko, R. L. Kurucz, R. Chornock, R. J. Foley, V. Stanishev, and R. Ibata, *Nature*, 2004, 431: 1069, arXiv: astro-ph/0410673
247. W. E. Kerzendorf, B. P. Schmidt, M. Asplund, K. Nomoto, P. Podsiadlowski, A. Frebel, R. A. Fesen, and D. Yong, *Astrophys. J.*, 2009, 701: 1665, arXiv: 0906.0982
248. W. E. Kerzendorf, B. P. Schmidt, J. B. Laird, P. Podsiadlowski, and M. S. Bessell, arXiv: 1207.4481, 2012

249. B. E. Schaefer and A. Pagnotta, *Nature*, 2012, 481(7380): 164
250. T. R. Marsh, G. Nelemans, and D. Steeghs, *Mon. Not. R. Astron. Soc.*, 2004, 350(1): 113, arXiv: astro-ph/0312577
251. Z. Han and R. F. Webbink, *Astron. Astrophys.*, 1999, 349: L17
252. T. D. Brandt, R. Tojeiro, É. Aubourg, A. Heavens, R. Jimenez, and M. A. Strauss, *Astron. J.*, 2010, 140: 804, arXiv: 1002.0848
253. K. Krisciunas, N. B. Suntzeff, P. Candia, J. Arenas, J. Espinoza, D. Gonzalez, S. Gonzalez, P. A. Höflich, A. U. Landolt, M. M. Phillips, and S. Pizarro, *Astron. J.*, 2003, 125: 166, arXiv: astro-ph/0210327
254. A. Pastorello, S. Taubenberger, N. Elias-Rosa, P. A. Mazzali, et al., *Mon. Not. R. Astron. Soc.*, 2007, 376(3): 1301, arXiv: astro-ph/0702566
255. A. Pastorello, P. A. Mazzali, G. Pignata, S. Benetti, et al., *Mon. Not. R. Astron. Soc.*, 2007, 377(4): 1531, arXiv: astro-ph/0702565
256. V. N. Gamezo, A. M. Khokhlov, and E. S. Oran, *Phys. Rev. Lett.*, 2004, 92: 211102, arXiv: astro-ph/0406101
257. F. K. Röpkke and W. Hillebrandt, *Astron. Astrophys.*, 2005, 431: 635, arXiv: astro-ph/0409286
258. T. Plewa, A. C. Calder, and D. Q. Lamb, *Astrophys. J.*, 2004, 612: L37, arXiv: astro-ph/0405163
259. M. Kromer, M. Fink, V. Stanishev, S. Taubenberger, F. Ciaraldi-Schoolman, R. Pakmor, F. K. Roepke, A. J. Ruiter, I. R. Seitenzahl, S. A. Sim, G. Blanc, N. Elias-Rosa, and W. Hillebrandt, arXiv: 1210.5243, 2012
260. G. C. IV Jordan, H. B. Perets, R. T. Fisher, and D. R. van Rossum, arXiv: 1208.5069, 2012
261. S. Yoon and N. Langer, *Astron. Astrophys.*, 2005, 435, 967, arXiv: astro-ph/0502133
262. M. Steinmetz, E. Muller, and W. Hillebrandt, *Astron. Astrophys.*, 1992, 254: 177
263. J. M. M. Pfannes, J. C. Niemeyer, and W. Schmidt, *Astron. Astrophys.*, 2010, 509: A75+, arXiv: 0911.3545
264. J. M. M. Pfannes, J. C. Niemeyer, W. Schmidt, and C. Klingenberg, *Astron. Astrophys.*, 2010, 509: A74+, arXiv: 0911.3540